



# TID climatologies in Antarctica and Europe derived from HF and GNSS observations

*Dima Paznukhov*





## Abstract

Traveling Ionospheric Disturbances (TIDs) attract significant attention of the ionospheric community. These propagating waves contribute to the energy exchange between different parts of the ionosphere and also affect high frequency (HF) radiowave propagation through the ionospheric plasma. Specialized techniques using GPS TEC and HF data have been developed for TID observations. Using a significant amount of the data collected in Antarctica and Europe statistical pictures of the TID occurrence in these regions are established. Overall the observed climatology of ionospheric disturbances varies significantly through the year and is mainly controlled by background plasma density distribution. There is a significant difference between daytime and night time disturbance characteristics as the former are controlled by the neutral wind parameters while the latter appear to be related to the electromagnetic processes in the ionosphere.

### ***Main contributors:***

***BC: K.Groves, K. Kraemer***

***Ebre Observatory: D. Altadill, E. Blanch***

***RINAN: V. Galushko, Yu. Yampolski, A. Koloskov, A. Sopin, A. Kacsheev***



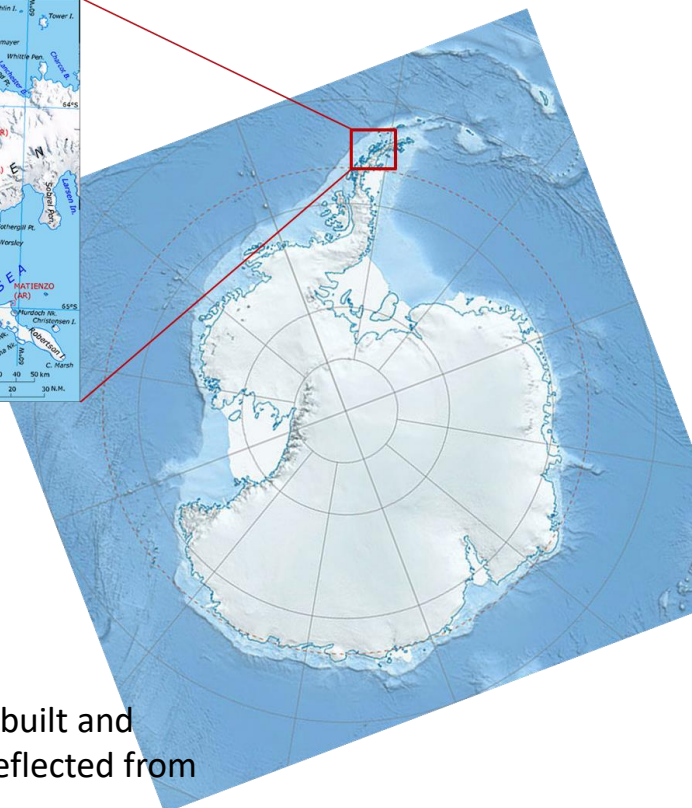
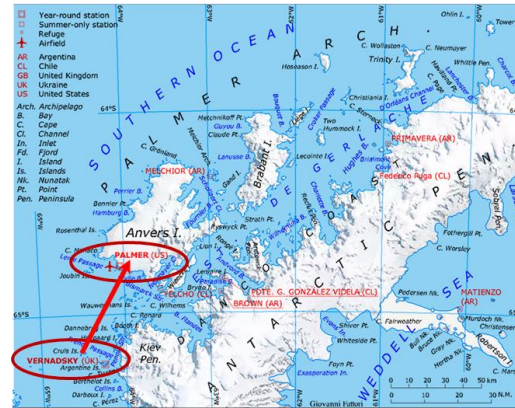
# Outline

- GNSS/HF study in Antarctica
- HF observations with Ebre digisonde (tilt measurements)
- HF observations in Europe (HF Interferometry)
- Summary



# TID observations at Vernadsky-Palmer

Drake Passage in Antarctica generates severe tropospheric waves, i.e., it is associated with cyclones, convective plumes, enhanced zonal winds, orographic waves, etc. This makes it a very good candidate for studying tropospheric-ionospheric interaction and propagation of the weather disturbances from the ground level to the ionospheric heights.



## Bistatic HF System

- Three-channel HF receive system based on software-defined radio built and installed at Palmer Station to measure parameters of HF signals reflected from ionosphere.
- Transmitter is installed at Vernadsky station (50 km due south).
- Raw data (decimated IQ samples) shipped by sea to Boston College

Parameter	Value	Comments
Operating frequency	2-10 MHz	appropriate for the location
Radiated power	< 50 W	CW
Output sample rate	100 Hz-1 kHz	reduces data storage requirements
Input Rx Impedance	50 Ohm	compatible standard
Operating system	Linux	real-time system

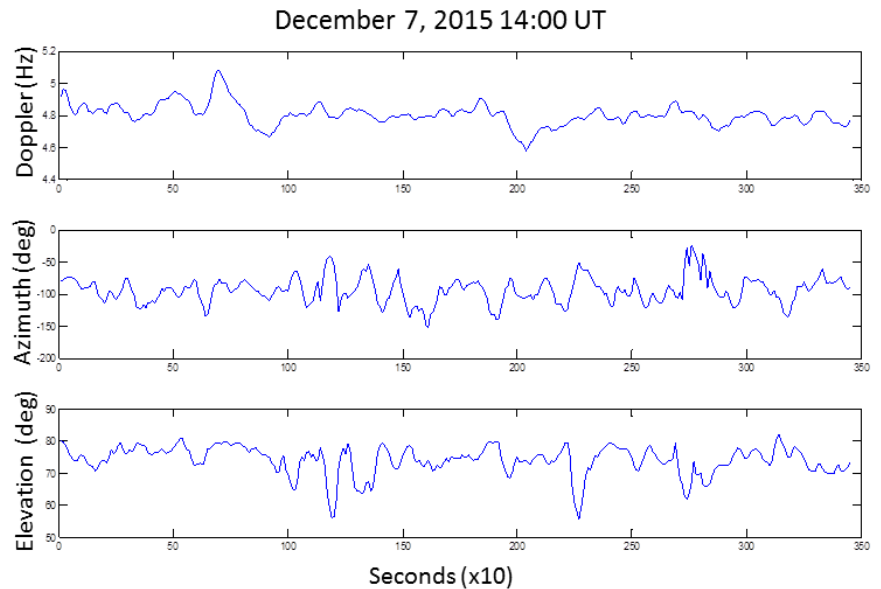


## Single Site System Characteristics

Parameter	Value	Comment
Operating frequency	2-15 MHz	appropriate for mid-latitudes
Radiated power	~ 1 kW	peak or CW; > 1000 km range
Total pulse width	~ 550 $\mu$ sec	16-chip code
Single chip length	~ 30 $\mu$ sec	time delay resolution
Output sample rate	100 Hz-1 kHz	reduces data file storage reqmnts
Receiver bandwidth	~30kHz	matched to chip length
Timing accuracy	$\leq 1 \mu$ sec	exceeds measurement reqmnts
Input Rx Impedance	50 Ohm	compatible standard
Operating system	Linux	real-time system

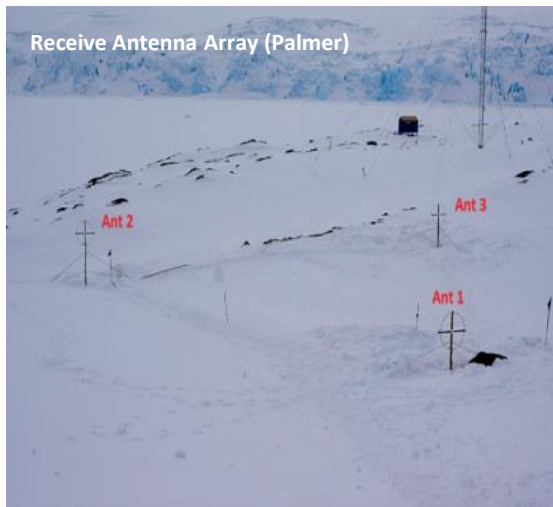
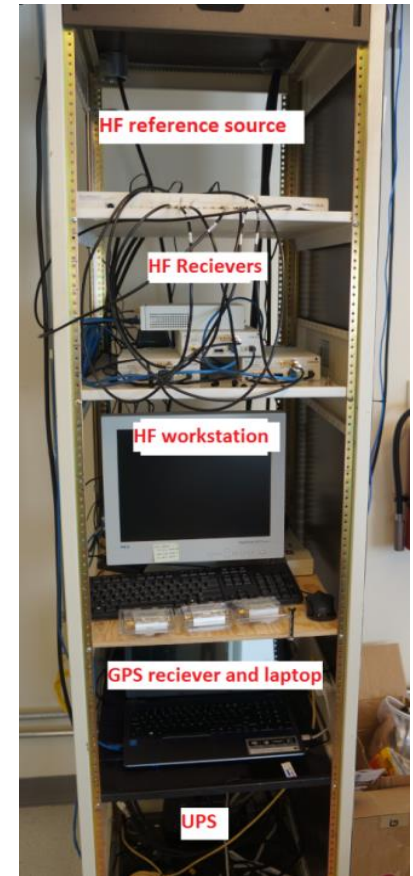
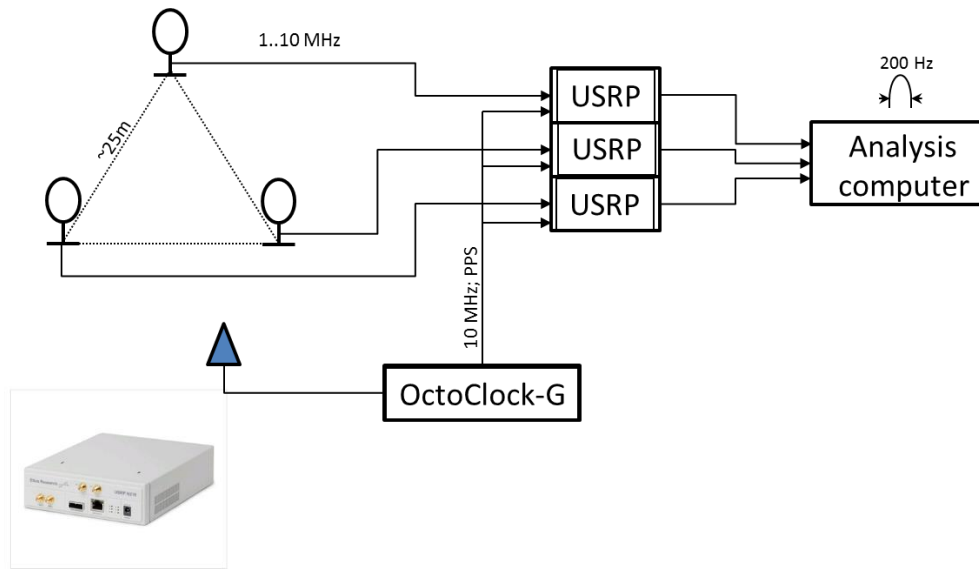
NTIDs measured signal parameters:

- AoA
- Time of Flight
- Doppler shift





# Existing Rx System at Palmer



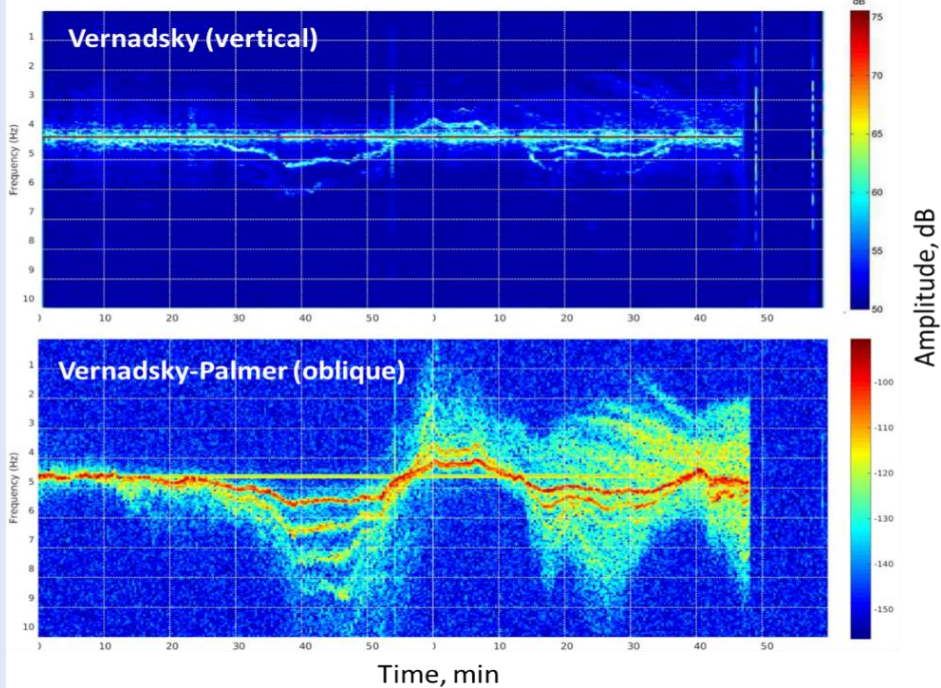
Three channel coherent HF receive system together with GNSS receiver

Receive antennas at Palmer



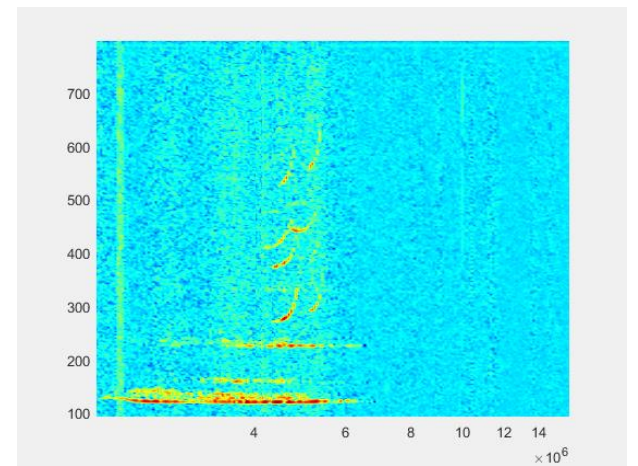
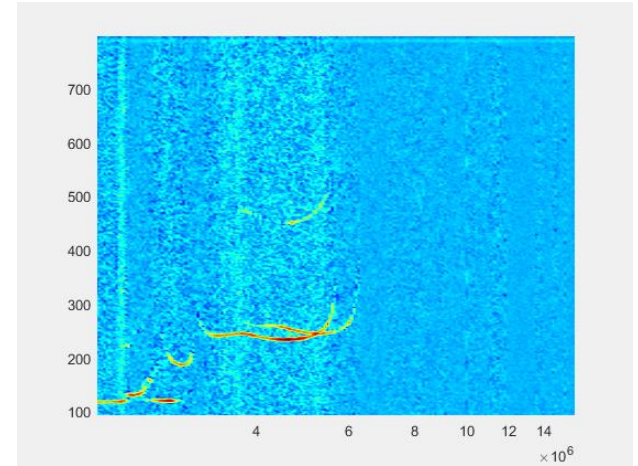
# Existing Tx System at Palmer

2016-03-15 22:00, Ch1, S/N = F44785



24

Oblique and vertical sounding, fixed frequency



Vertical sounding, frequency sweep (ionogram)  
at Vernadsky

(Zalizovsky et al., 2018)



## Existing Tx System at Palmer

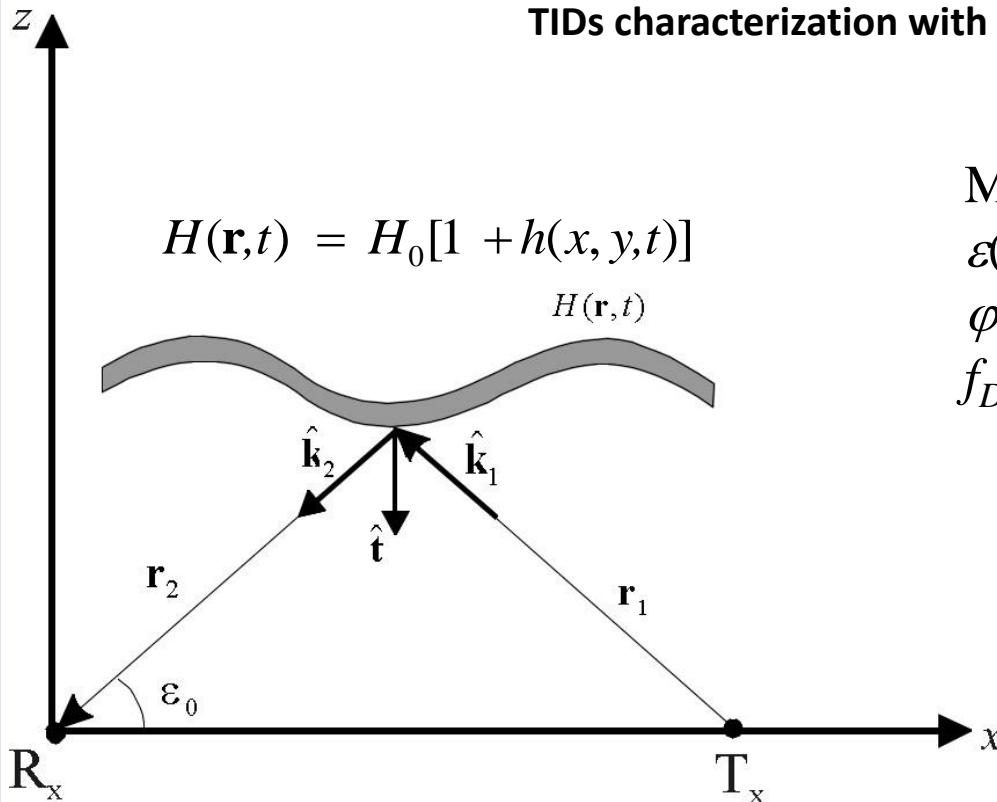


Transmitter assembly at Vernadsky station. The system includes ICOM-718 transceiver, antenna tuner, power supply box, modulator, and PC computer. Operational power  $\sim 30$  W.





## TIDs characterization with FAS technique



Perfectly reflecting surface model

Surface spectral representation:

$$h(x, y, t) = \int_{-\infty}^{\infty} N(\Omega) e^{i\Omega t} d\Omega e^{-iK(\Omega)(x \cos \theta(\Omega) + y \sin \theta(\Omega))}$$

$N(\Omega)$  – TID amplitude

$K(\Omega)$  – TID wavenumber

$\theta(\Omega)$  – TID direction of motion

Measured signal parameters:

$\varepsilon(t)$  elevation angle

$\varphi(t)$  azimuthal angle

$f_D(t)$  Doppler shift

Spectral representations:

$$\varepsilon(t) = \int_{-\infty}^{\infty} S_{\varepsilon}(\Omega) e^{i\Omega t} d\Omega$$

$$\varphi(t) = \int_{-\infty}^{\infty} S_{\varphi}(\Omega) e^{i\Omega t} d\Omega$$

$$f_D(t) = \int_{-\infty}^{\infty} S_F(\Omega) e^{i\Omega t} d\Omega$$

$$\varepsilon(t), \varphi(t), f_D(t) \Leftrightarrow h(x, y, t)$$

(Beley et al, 1995; Paznukhov et al, 2012)



## FAS solution

With the use of the spectral representation, one gets solutions

Trajectory parameters spectra: (direct problem)

$$S_{\varepsilon}(\Omega) = N(\Omega)[\sin \varepsilon_0 \cos \varepsilon_0 - iH_0 K(\Omega) \cos \theta(\Omega)]$$

$$S_{\varphi}(\Omega) = iH_0 K(\Omega) N(\Omega) \tan \varepsilon_0 \sin \theta(\Omega)$$

$$S_F(\Omega) = -2iH_0 \Omega N(\Omega) \sin \varepsilon_0 / \lambda$$

Reflecting surface spectra: (inverse problem)

$$N(\Omega) = \frac{i\lambda S_F(\Omega)}{2H_0 \Omega \sin \varepsilon_0}$$

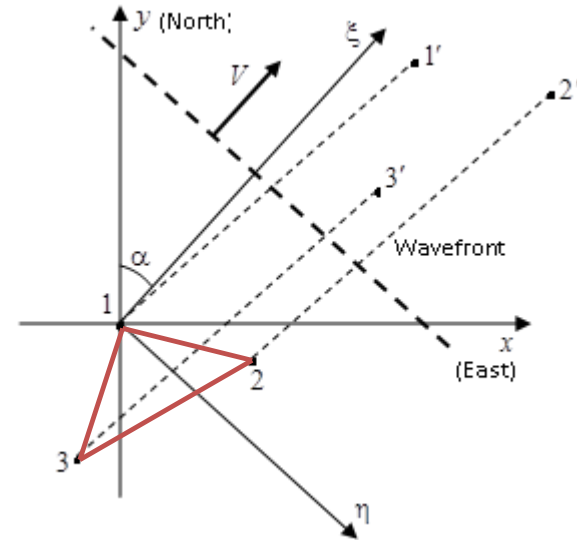
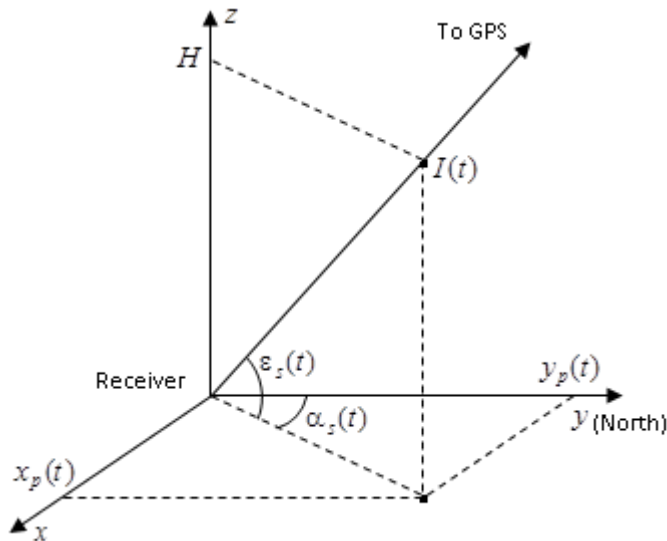
$$\tan \theta(\Omega) = -\frac{2H_0 \Omega \operatorname{Re} S_{\varphi}(\Omega)}{2H_0 \Omega \operatorname{Re} S_{\varepsilon}(\Omega) \tan \varepsilon_0 + \lambda \operatorname{Im} S_F(\Omega) \sin \varepsilon_0}$$

$$K(\Omega) = -\frac{2\Omega \operatorname{Im} S_{\varphi}(\Omega) \cos \varepsilon_0}{\lambda \operatorname{Im} S_F(\Omega) \sin \theta(\Omega)}$$



# GNSS interferometry methods

(Afraimovich et al., 1998; Valladres and Hei, 2012; Galushko et al., 2016)



For any disturbance, represented as  $I(x, y, t) = I(x \sin \alpha + y \cos \alpha - Vt)$

Solution is:

$$V(t) = \frac{1}{\gamma(t)} \left[ \gamma_x(t) \frac{dx_p(t)}{dt} + \gamma_y(t) \frac{dy_p(t)}{dt} - I'(t) \right]$$

$$\sin \alpha(t) = \gamma_x(t) / \gamma(t) \quad \cos \alpha(t) = \gamma_y(t) / \gamma(t)$$

$$\gamma(t) = \pm \sqrt{\gamma_x^2(t) + \gamma_y^2(t)}$$

Where space and time derivatives are:

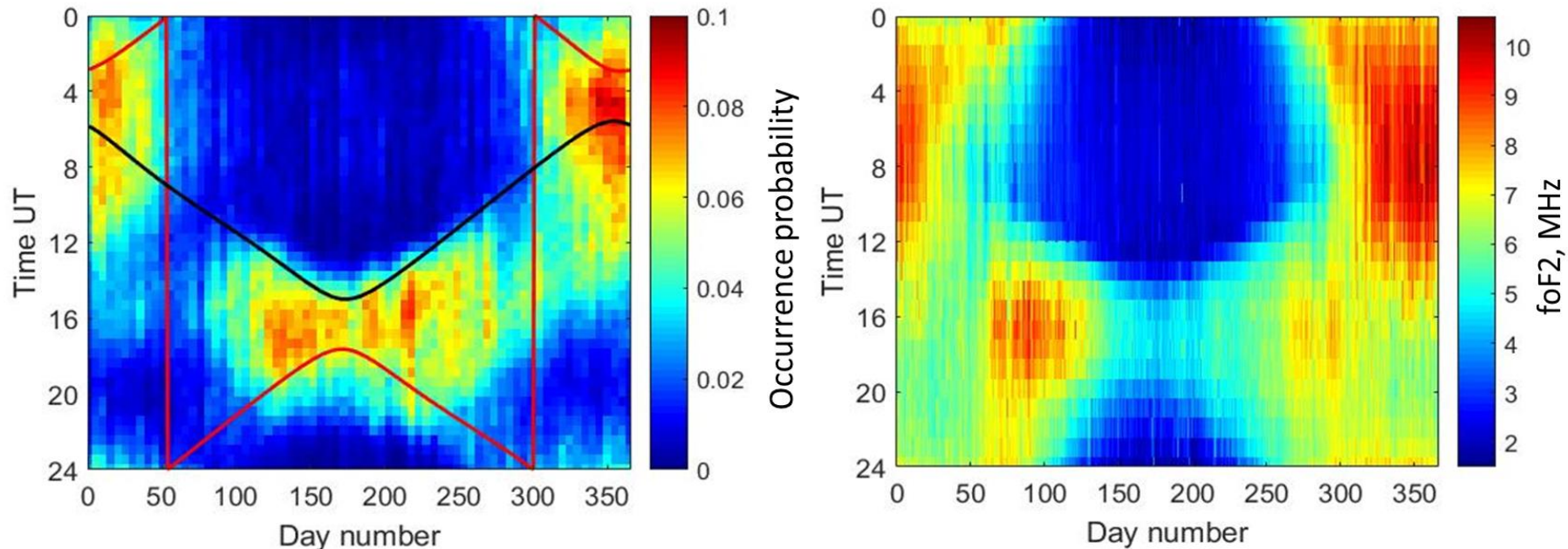
$$I'(t) = dI(x, y, t) / dt$$

$$\gamma_x(t) \equiv \partial I(x, y, t) / \partial x$$

$$\gamma_y(t) \equiv \partial I(x, y, t) / \partial y$$



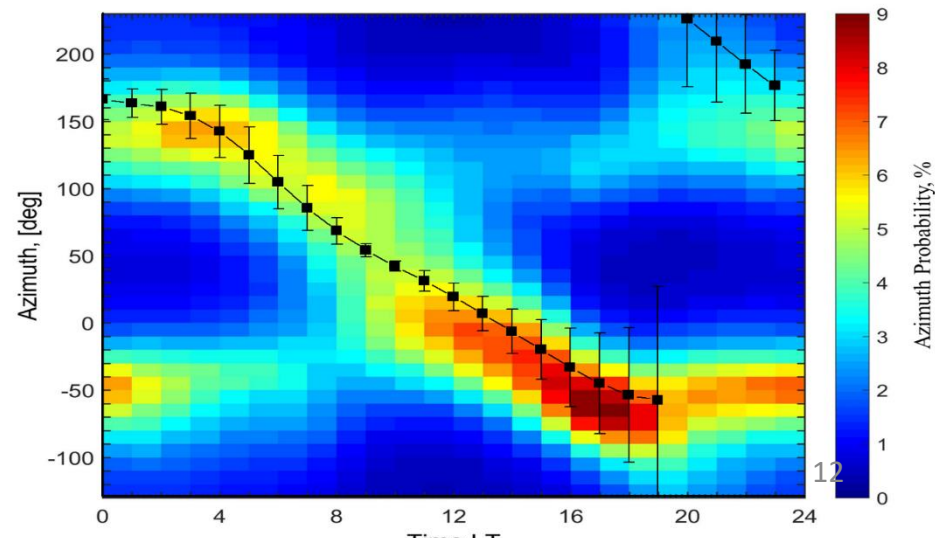
## Observed TID climatology 2009-2015 (GNSS)



Climatology of the observed TIDs. Left: TID climatology measured with GNSS TEC technique during 2009-2015.

Right: Plasma density distribution (in terms of foF2) during the same period measured with the ionosonde at Vernadsky. HF observations show that during the Antarctic summer time, TIDs are predominantly observed during the night time, when the local peak density is at its maximum (Weddell Sea Anomaly). Such plasma distribution is illustrated with the data from Vernadsky ionosonde. Therefore, TID intensity is directly proportional to the background plasma density. It is also worth noting that HF measurements show more disturbances during the night time.

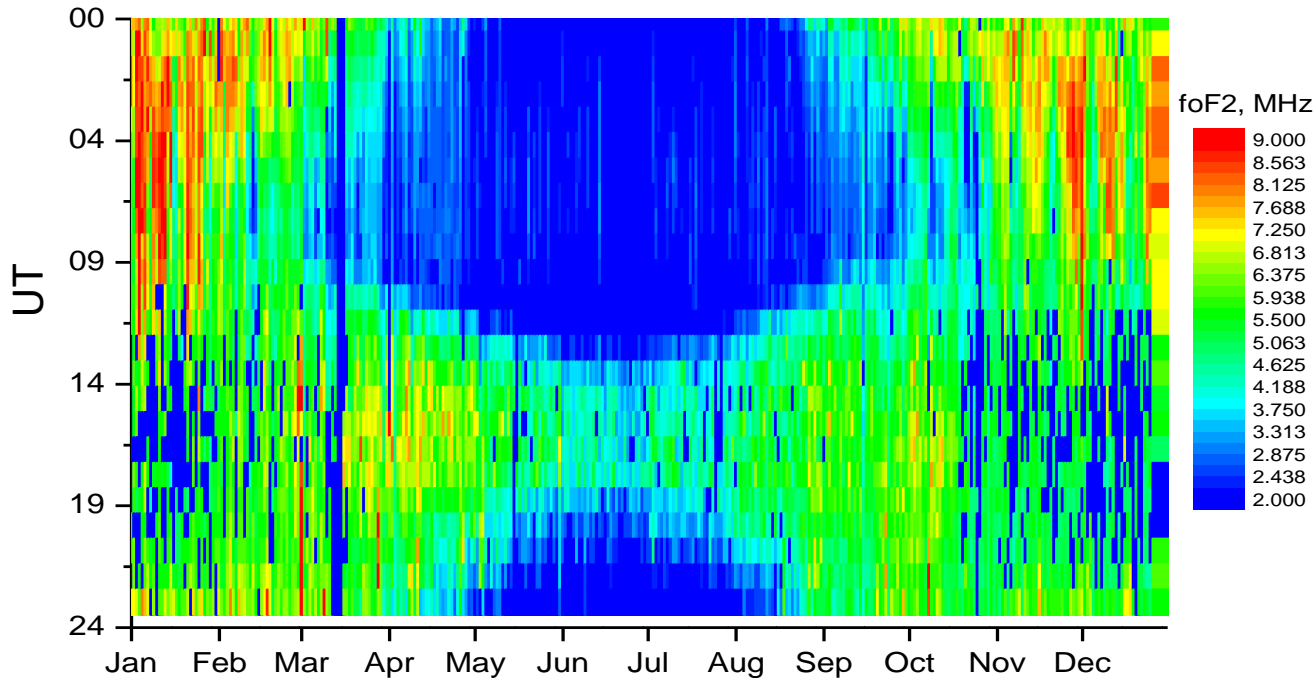
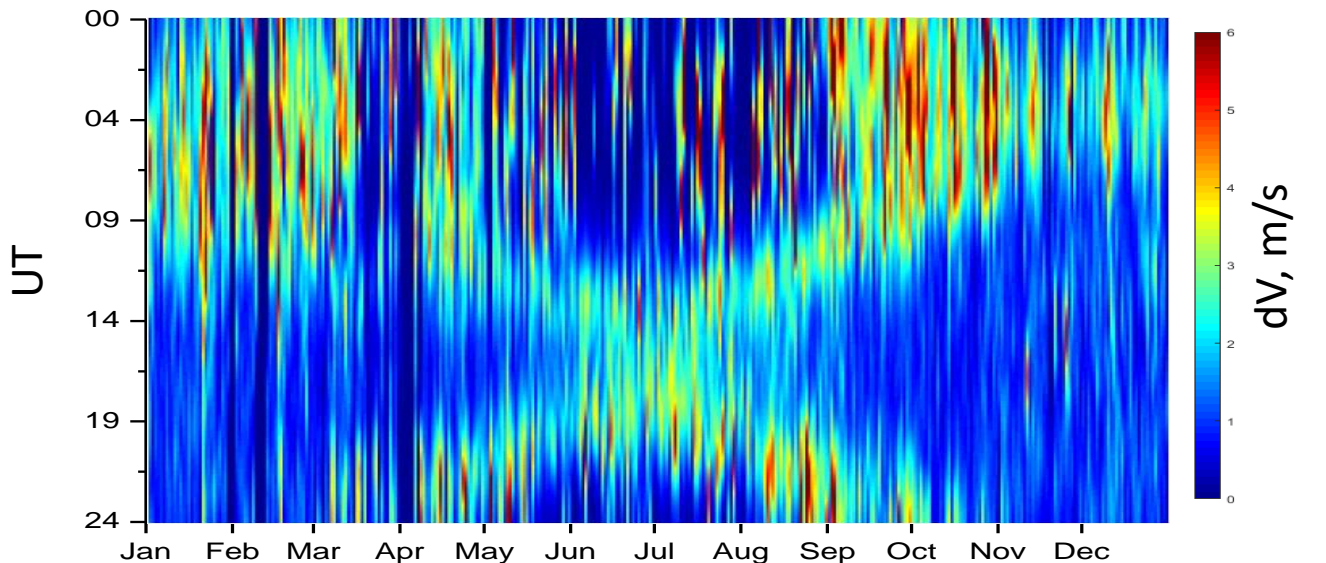
Bottom Right: “Perfect anti-match” between measured TID azimuth and modeled neutral wind direction (dots). The neutral wind is calculated with TIEGCM model. In the figure the direction of the neutral wind is shifted by 180 deg, thus showing the “anti-windward” direction. Quiet-time TID measurements for the entire period of observations are shown. Note that several TID modes are present simultaneously: one with changing azimuth and at least two others with constant azimuthal directions of about -50 deg and 150 deg.



(Paznukhov et al., JGR submitted 2019)

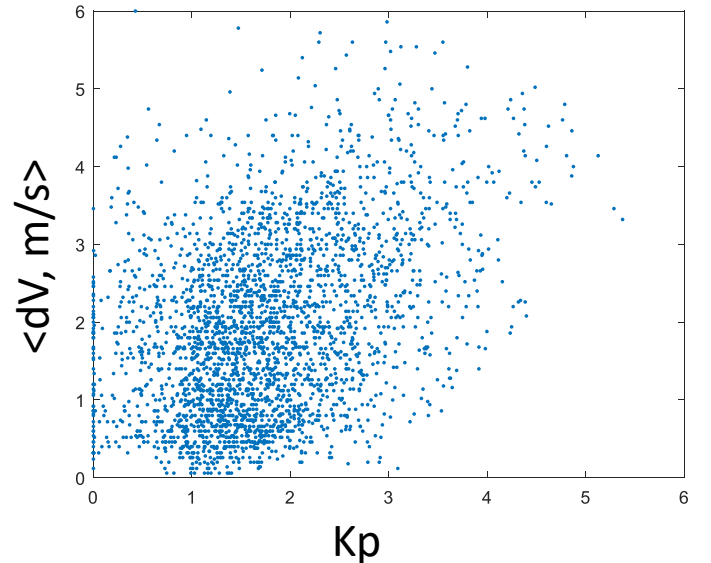
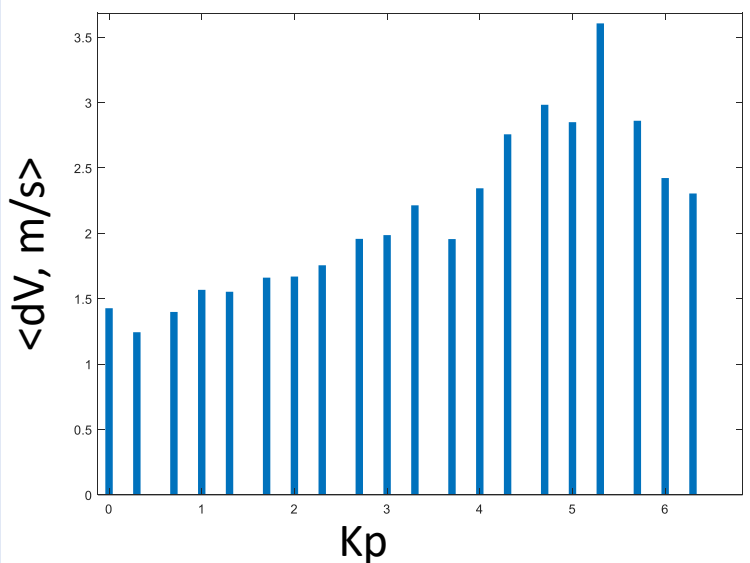
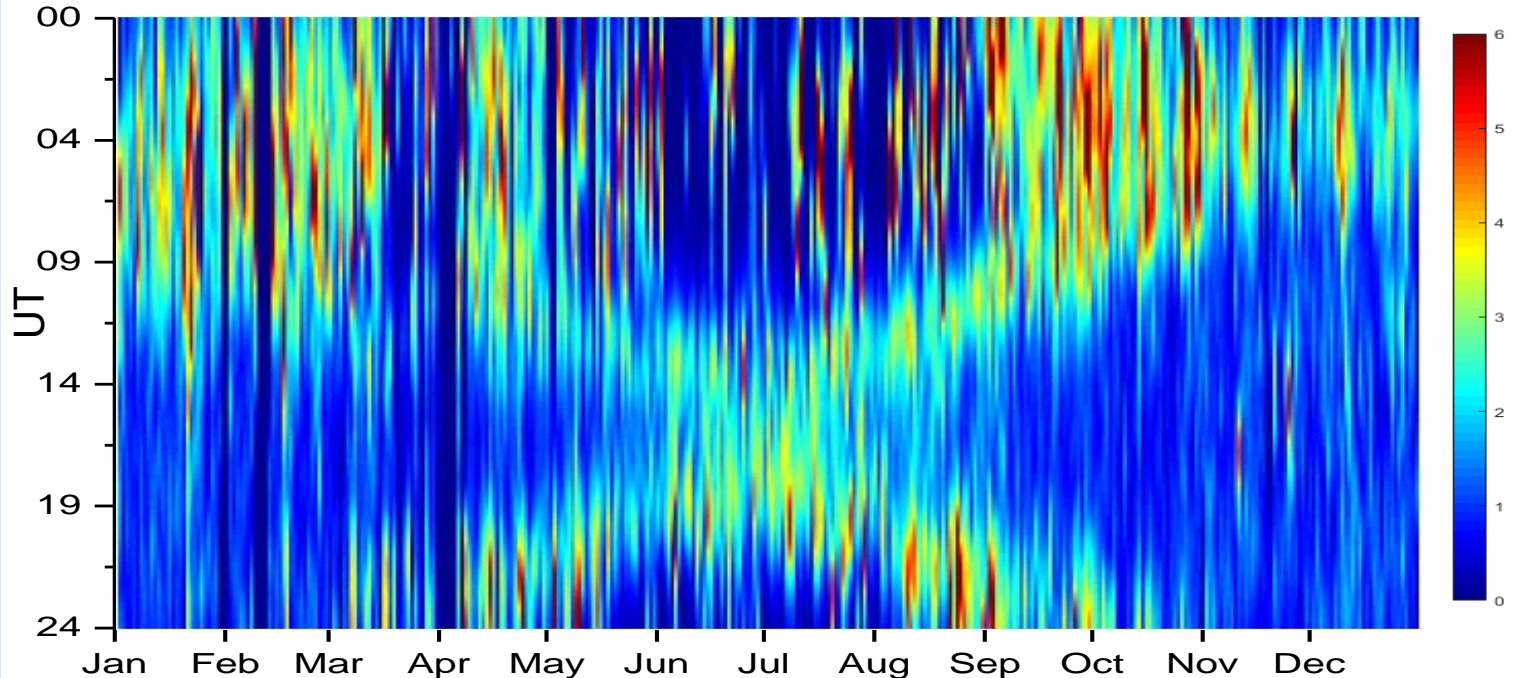


# #1 factor for TID occurrence is background electron density



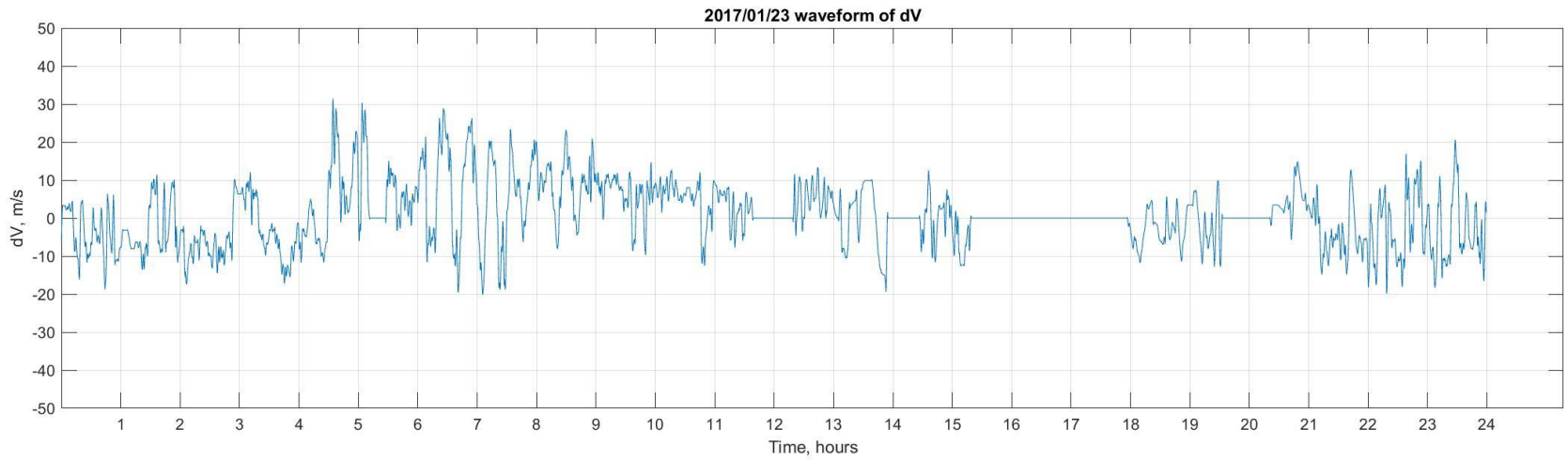
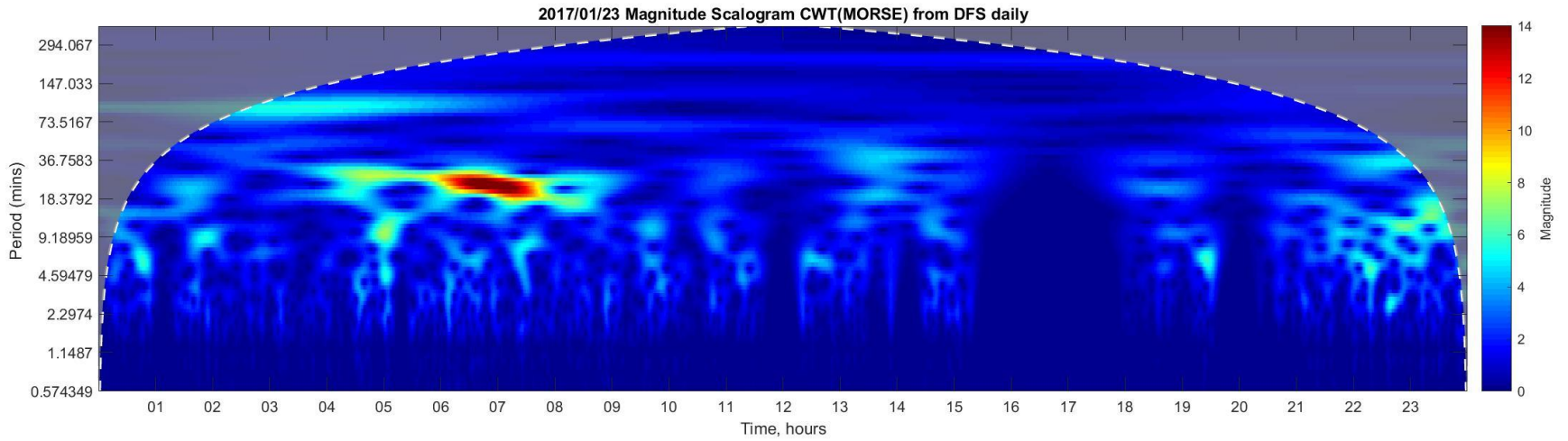


## #2 factor for TID occurrence is magnetic activity





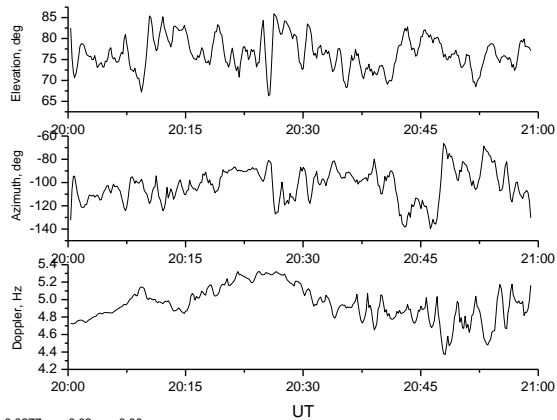
# Some Results collected from Vernadsky-Palmer link





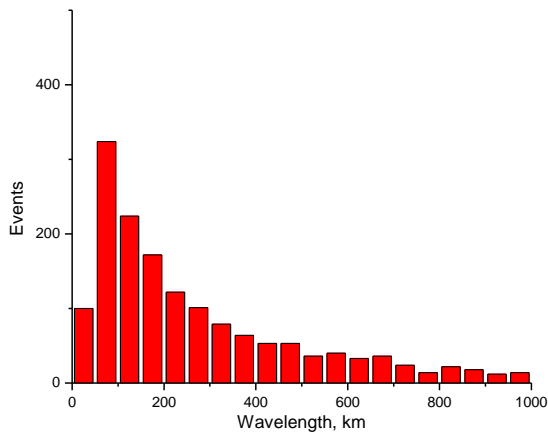
# Results of TID observations

Disturbances in the ionosphere (e.g., TIDs) affect the propagation of the HF radio waves. By measuring the parameters of the ionospherically reflected HF signal it is possible to monitor and to measure the characteristics of TIDs. Here the Frequency and Angular Sounding (FAS) method is used

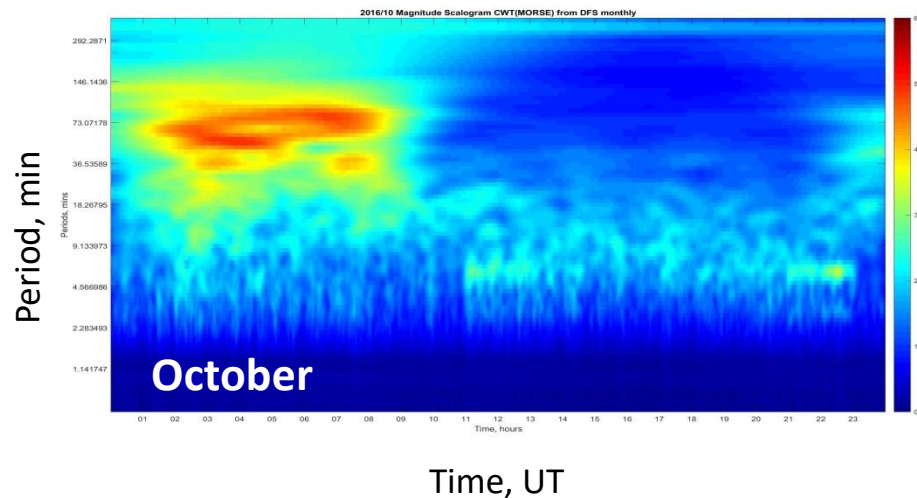
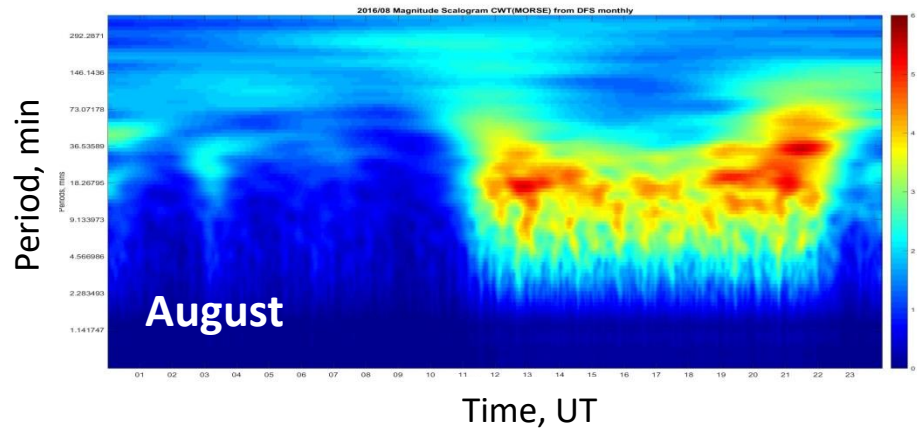


$p_{1,2}=0.0277$   $p_{1,3}=0.03$   $p_{2,3}=0.00$

Examples of the measured signal characteristics.



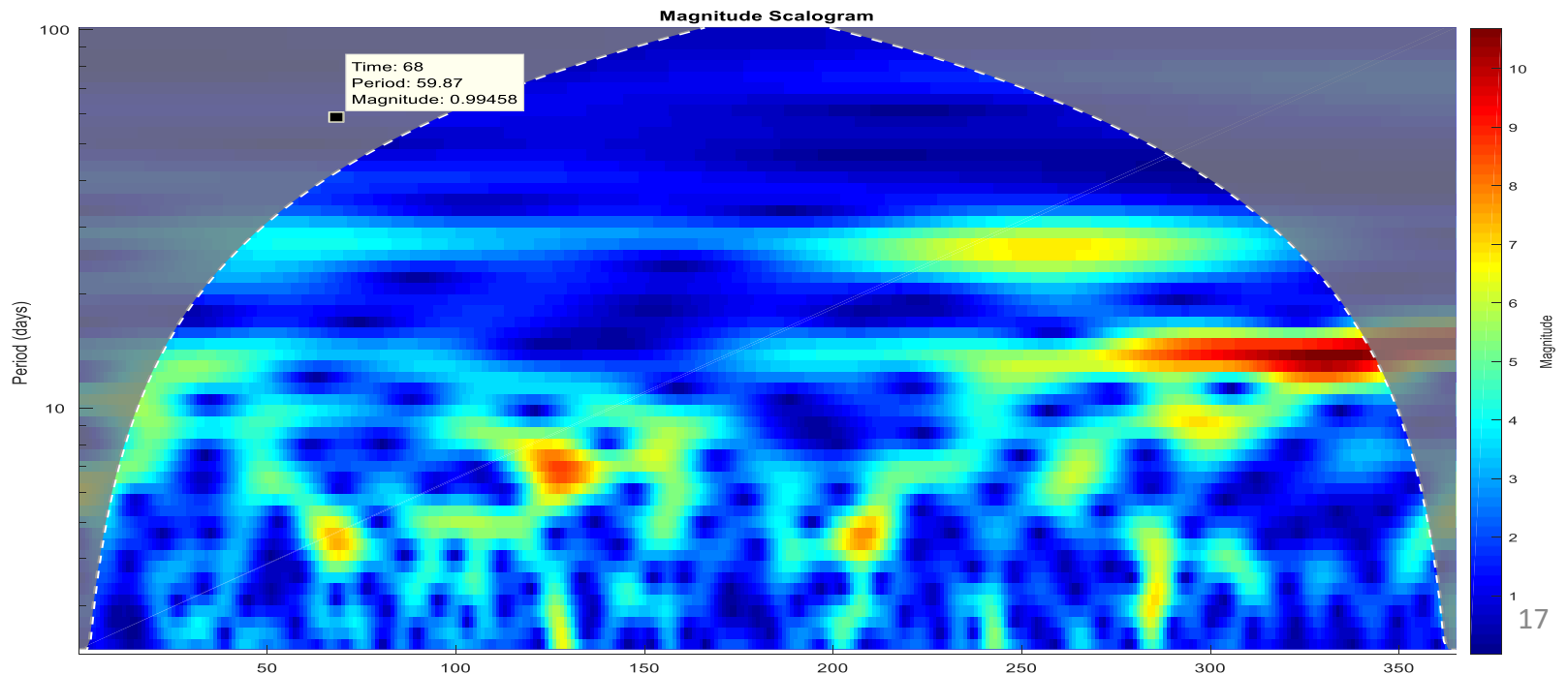
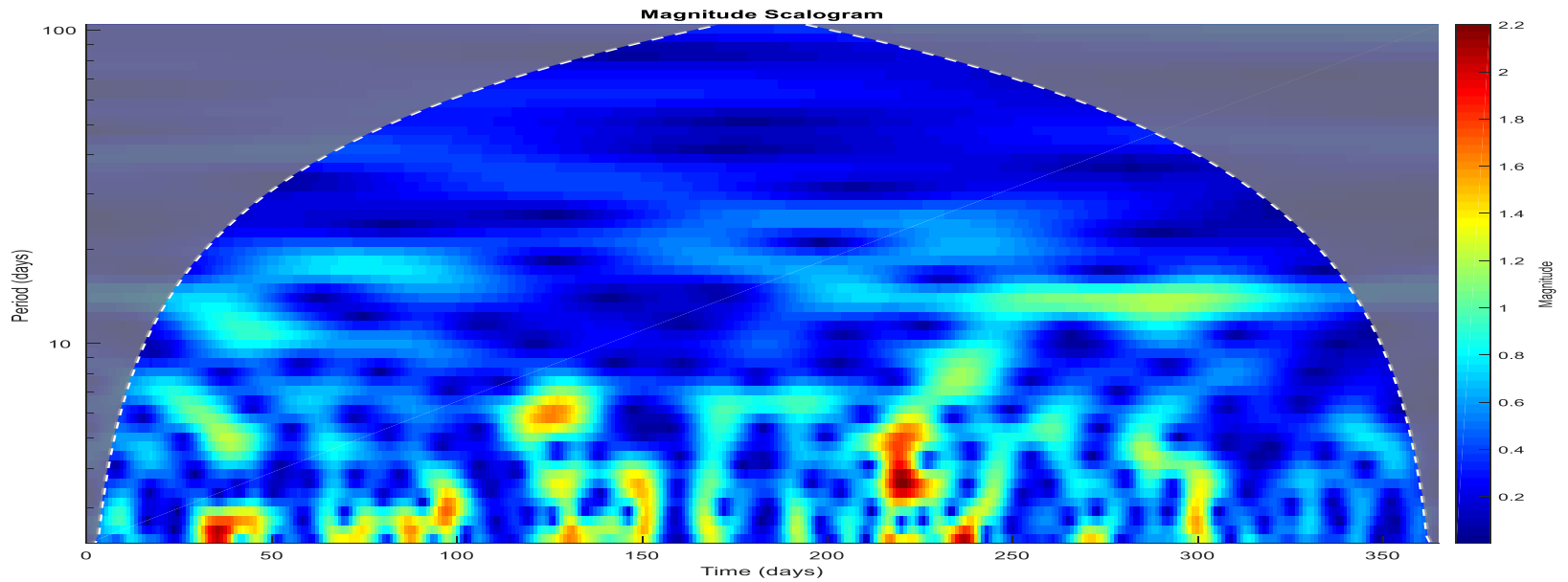
TID wavelengths observed from December 2015 to March 2016.



TID occurrence and characteristics vary significantly over the seasons. Top plot shows monthly averaged observations during the summer time, and bottom one near the equinox. During the summer TIDs are present during the night and have longer periods than those observed in October. Color scale shows intensity of variations.

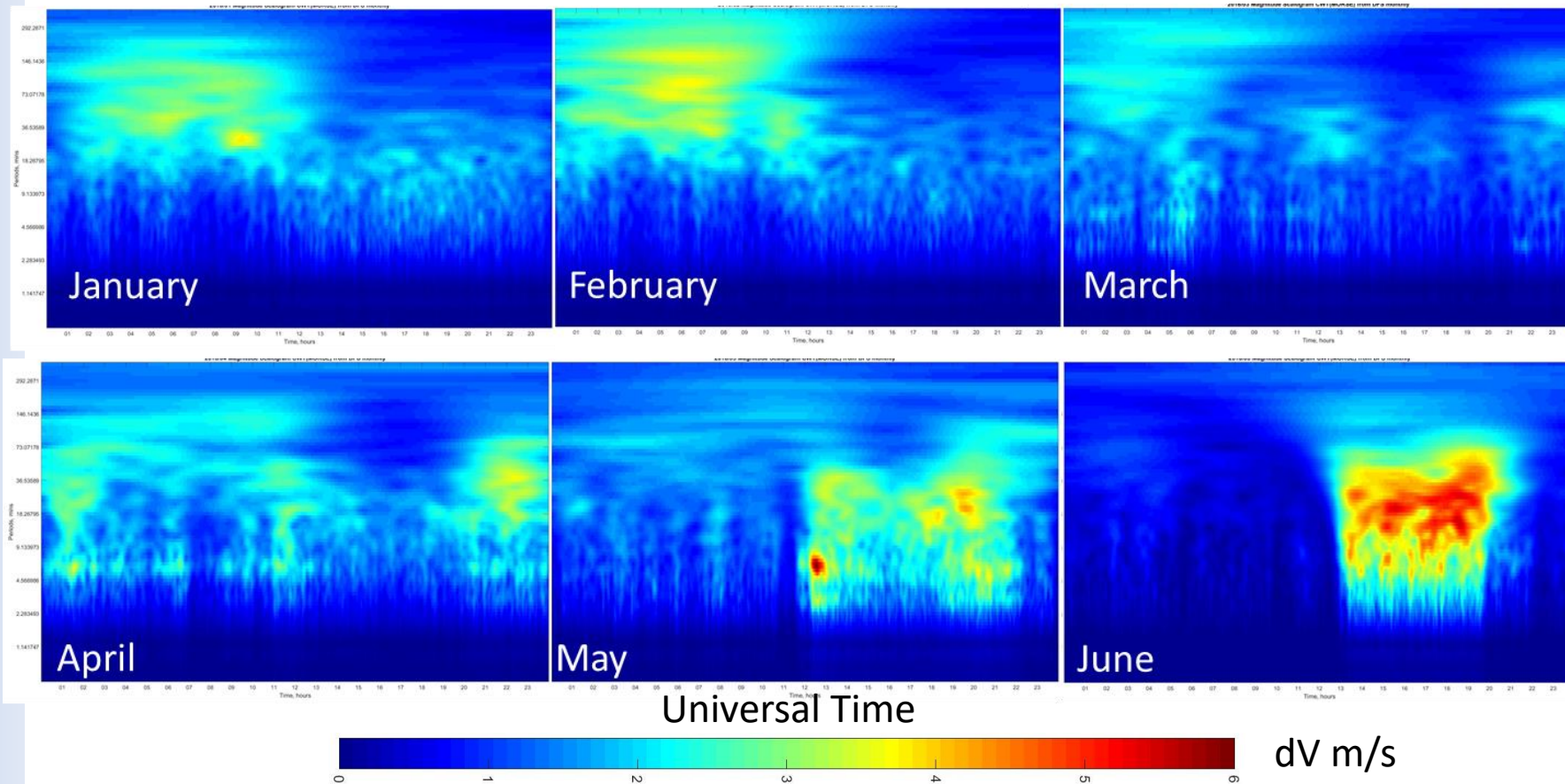


## #2 factor for TID occurrence is magnetic activity





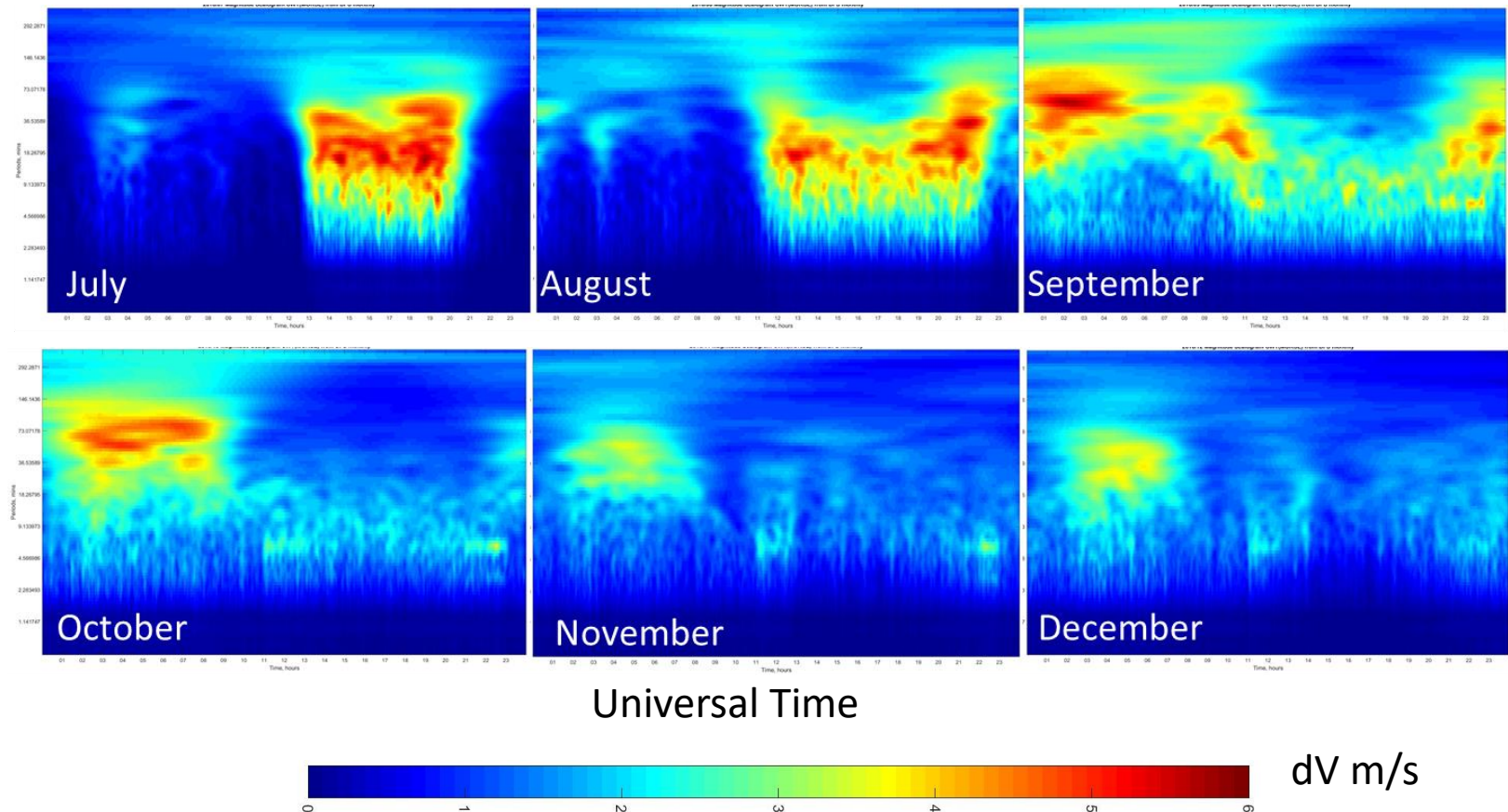
# Observed TIDs Climatology I



Seasonal distribution of the TIDs observed in 2016. The strongest amplitudes are observed during the periods with the high background plasma density. This corresponds to the daytime (around 13-19 UT) in the Antarctic winter (June solstice) and to nighttime (around 02-07 UT) in the summer (December solstice). The periods observed in the summer (30-140 min) are much longer than the wintertime ones (10-50 min).

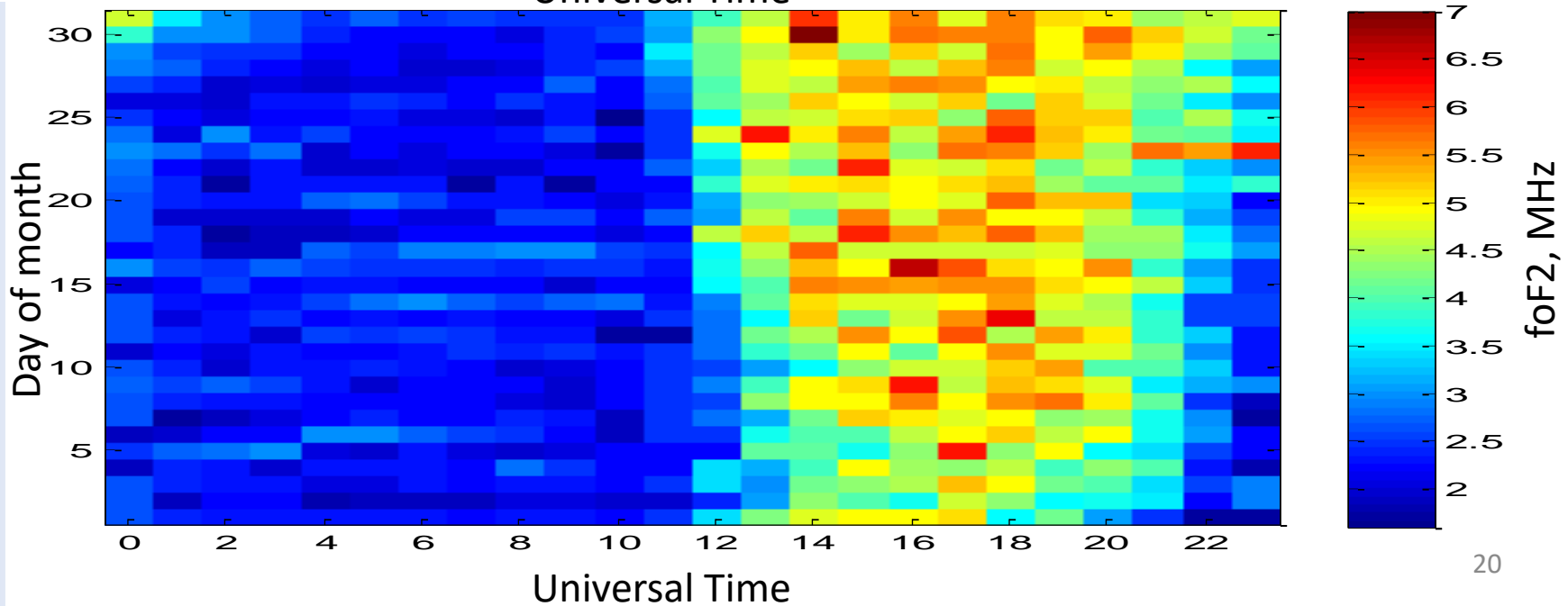
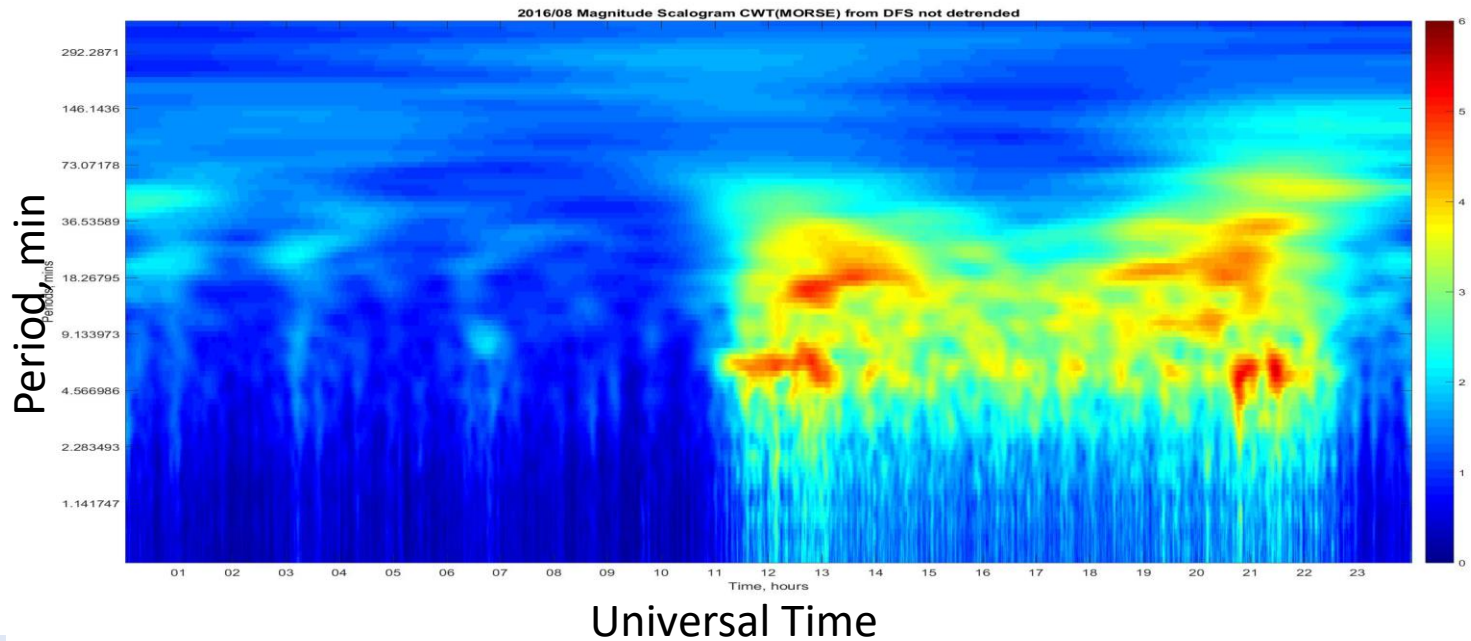


## Observed TIDs Climatology II



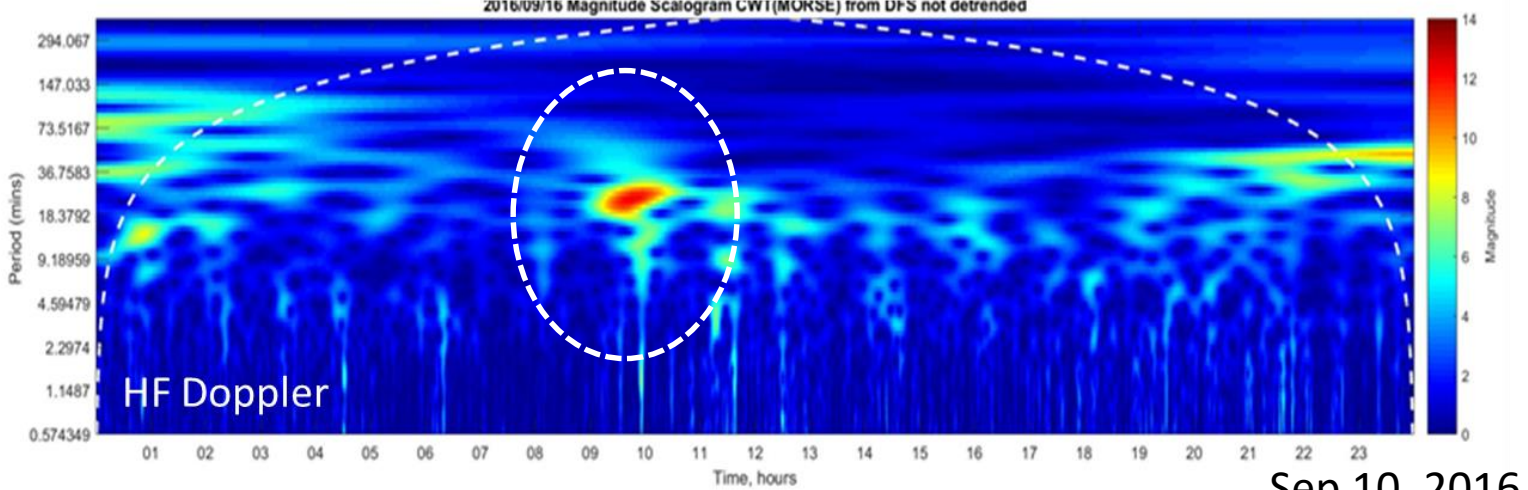
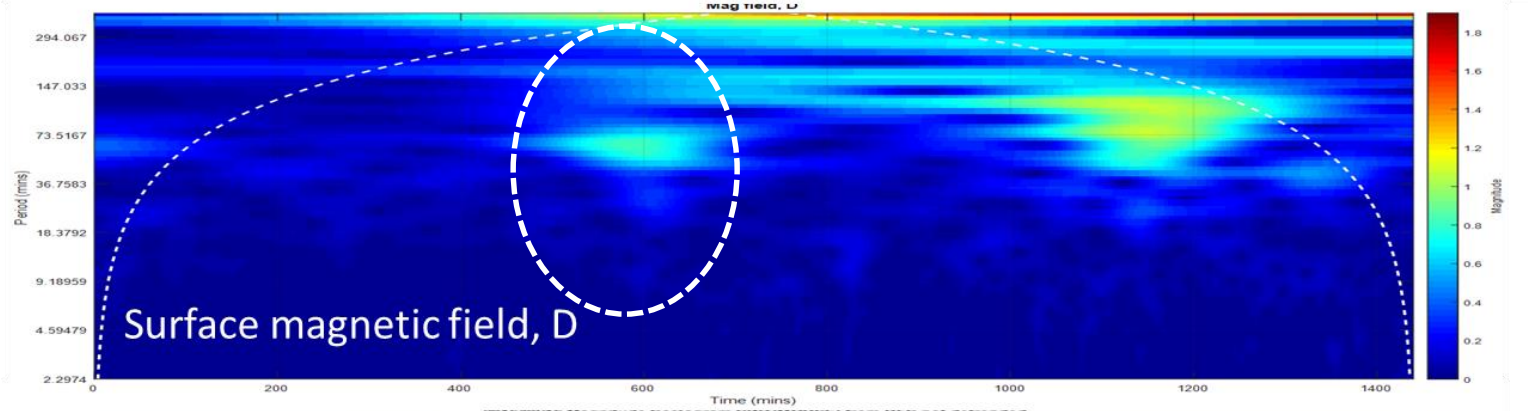
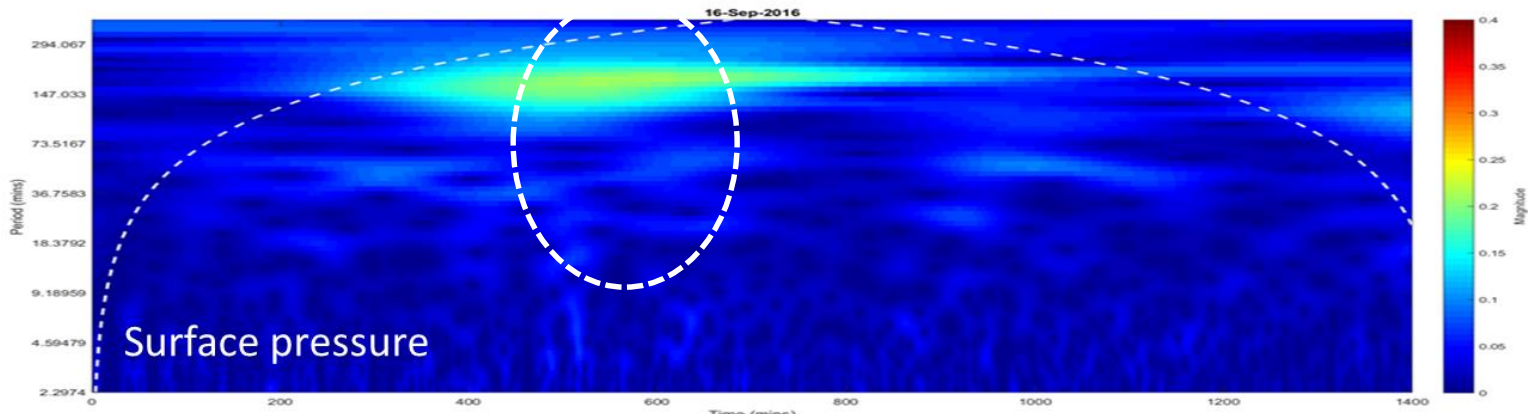
Seasonal distribution of the TIDs observed in 2016. The strongest amplitudes are observed during the periods with the high background plasma density. This corresponds to the daytime (around 13-19 UT) in the Antarctic winter (June solstice) and to nighttime (around 02-07 UT) in the summer (December solstice). The periods observed in the summer (30-140 min) are much longer than the wintertime ones (10-50 min).

# Observed TIDs Climatology I



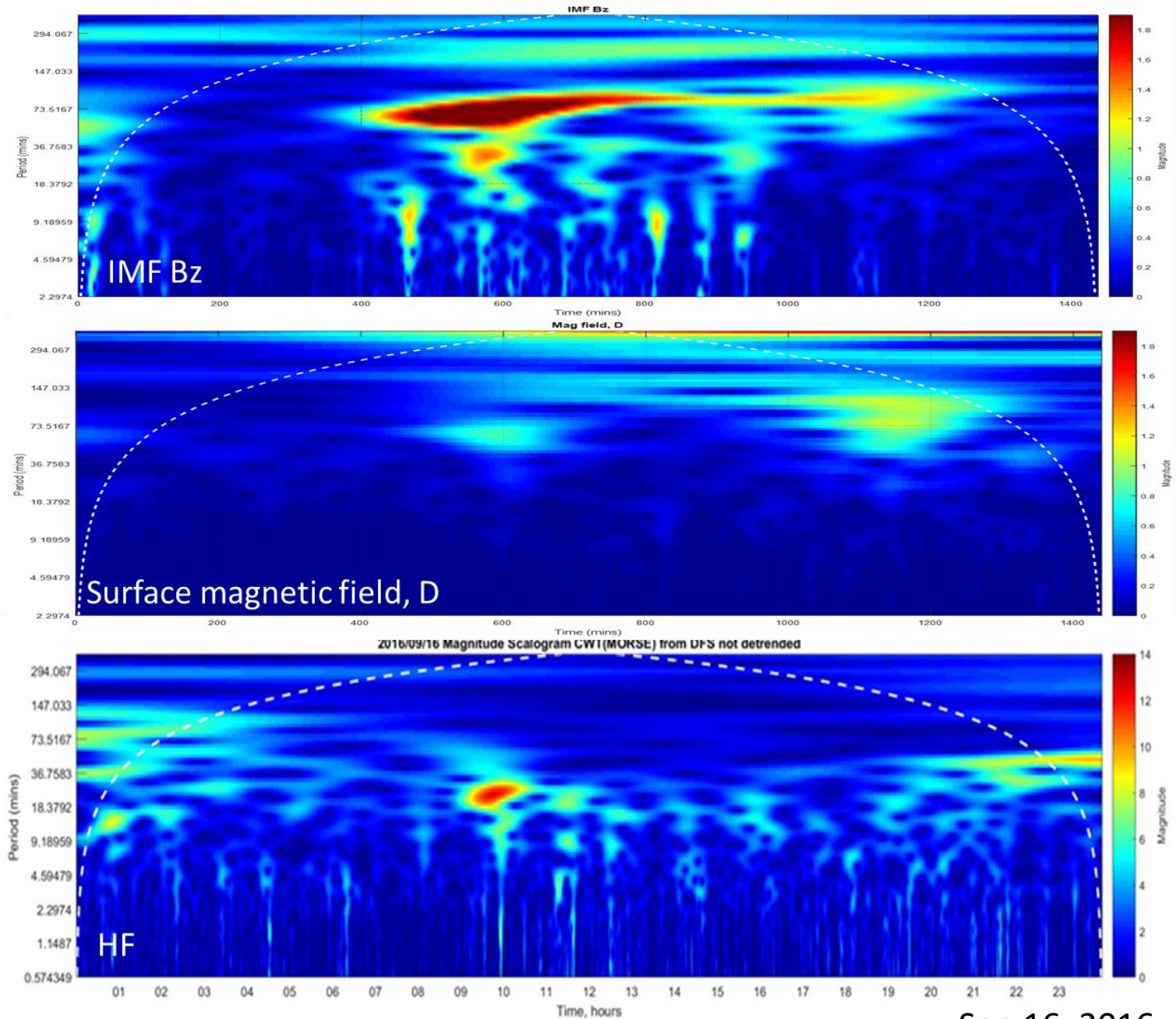


# How big a factor is the troposphere?

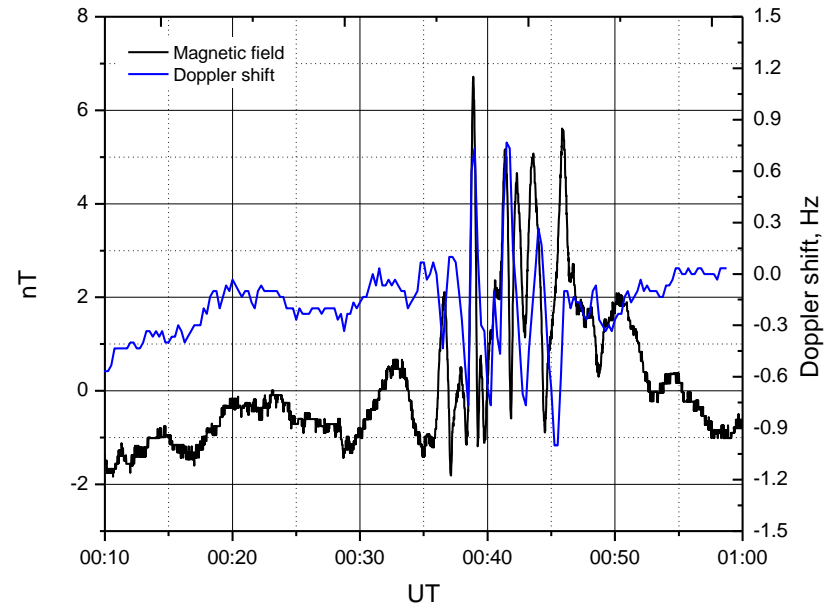
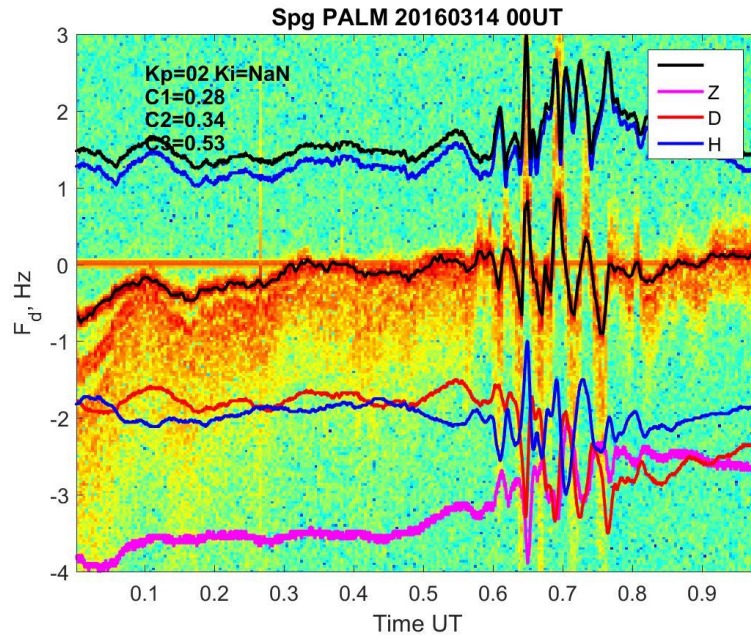




# Is magnetosphere a factor?



# Other phenomena observed by HF system



Left: Spectrogram of HF signal at Palmer together with H, D, Z and HD (horizontal) component of Earth magnetic field measured at Vernadsky magnetic observatory. Right: Comparison of the magnetic HD component variations to the Doppler shift of the maximum in the signal spectrum. Variations show the same periodicity and time of occurrence indicating that HF signal propagation is affected by the ULF geomagnetic field disturbances (Pc 3-5 band).



## Summary of the findings from Vernadsky-Palmer link

**#1 factor for TID occurrence is background electron density**

**#2 factor for TID occurrence is geomagnetic activity**

**#3 factor for TID occurrence is season**

**TID characteristics:**

**Summertime:**

**Occur during the night, with the periods 30-140 min**

**Wintertime:**

**Occur during the day, with the periods 10-50 min**





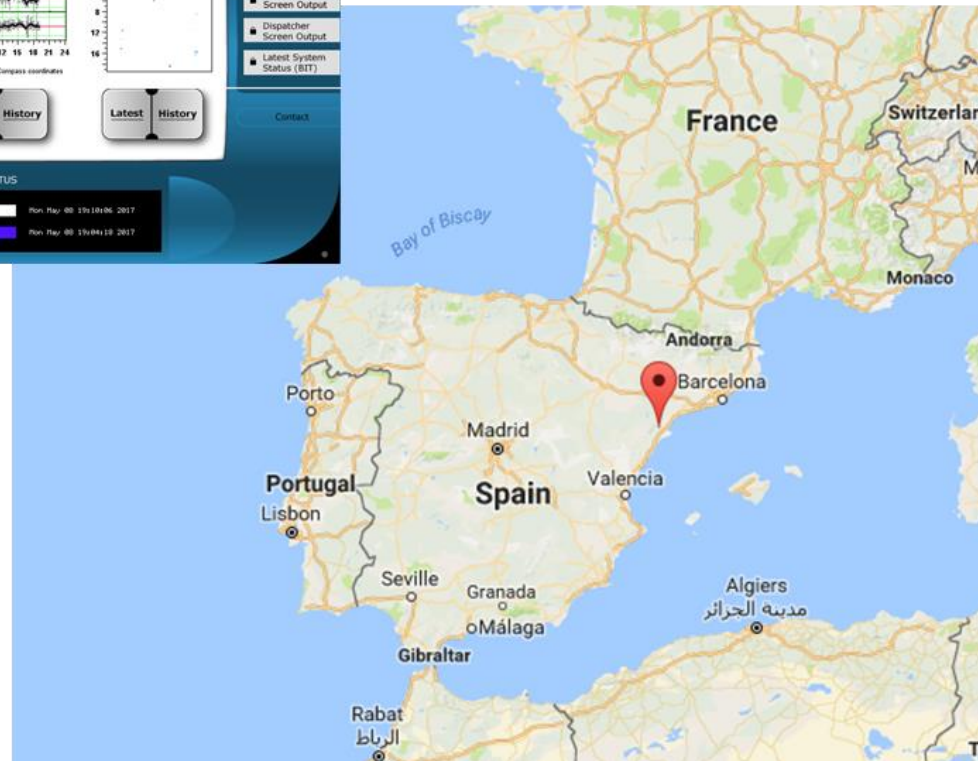
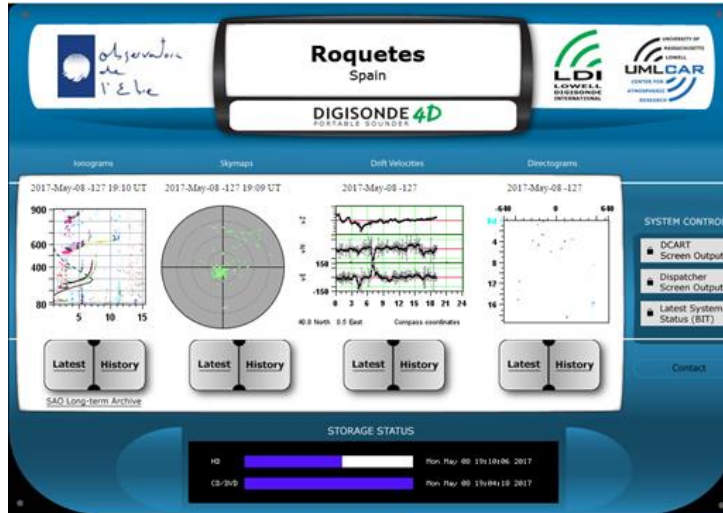
# HF observations with Ebro digisonde (tilt measurements)



*The Observatori de l'Ebre is a Research Institute founded by the Society of Jesus in 1904 to study Sun-Earth relationships.*

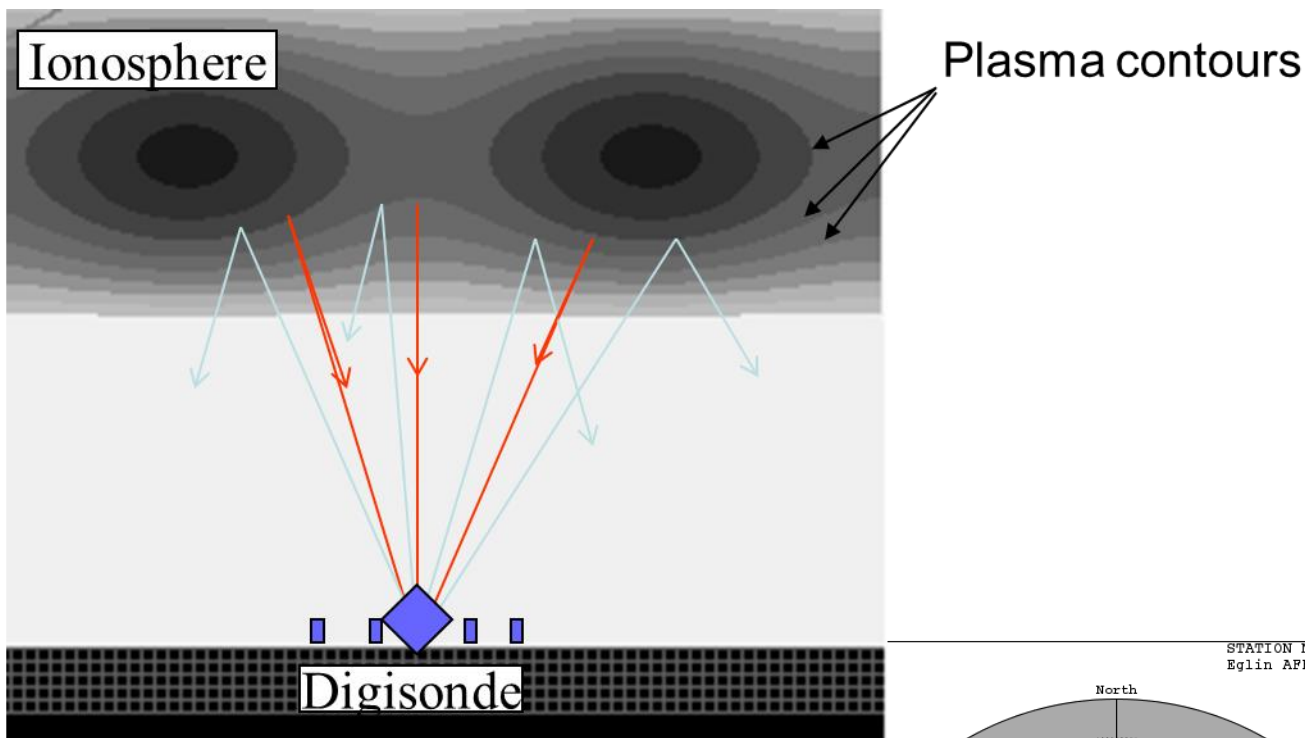


# Measurements at Ebro/Roquetes digisonde station

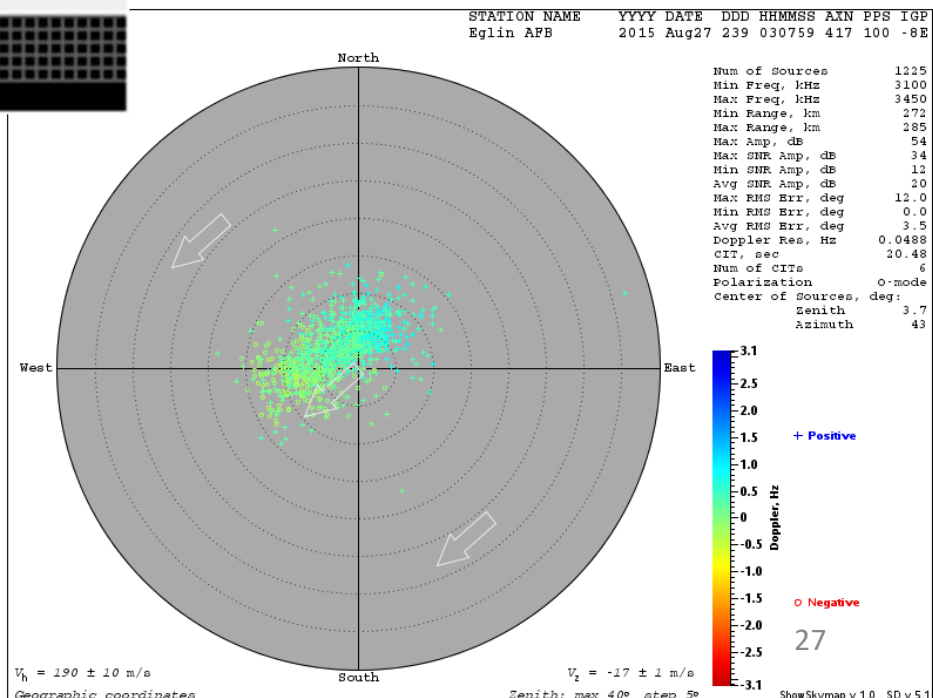




# Digisonde Tilt measurements

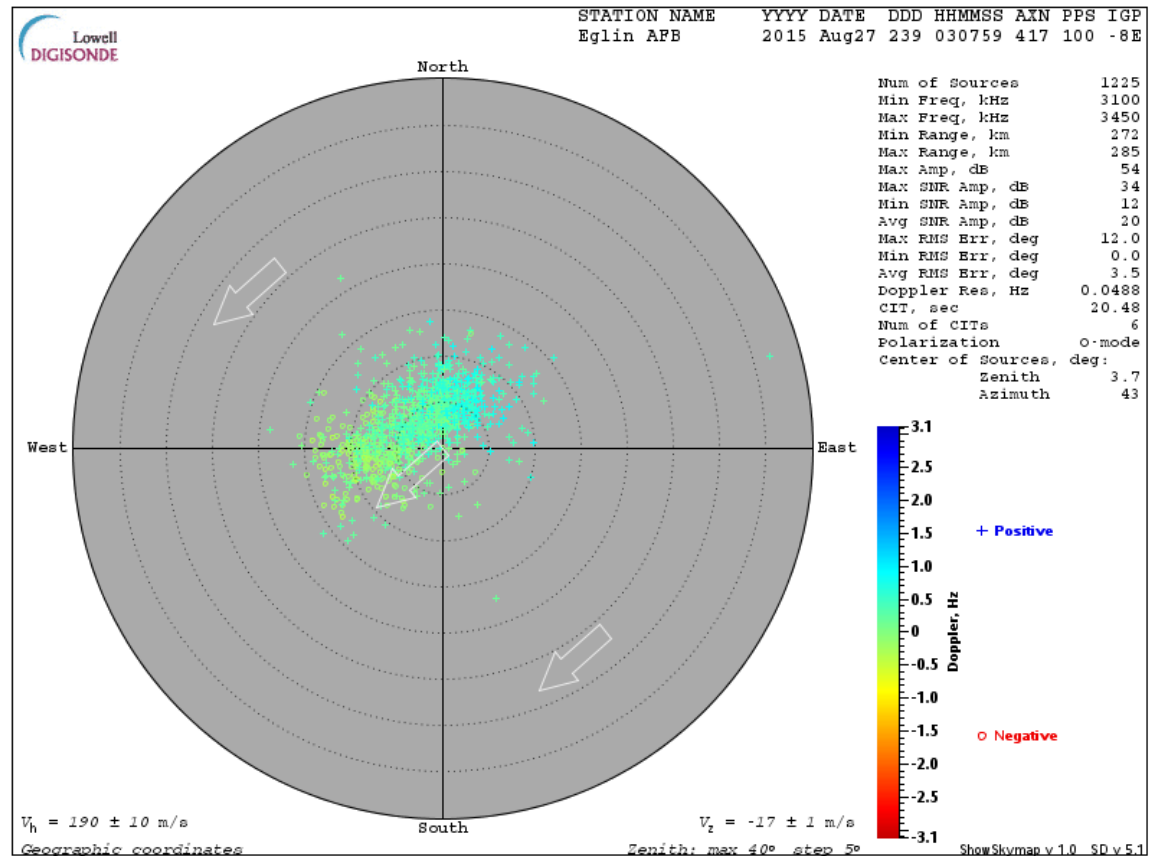
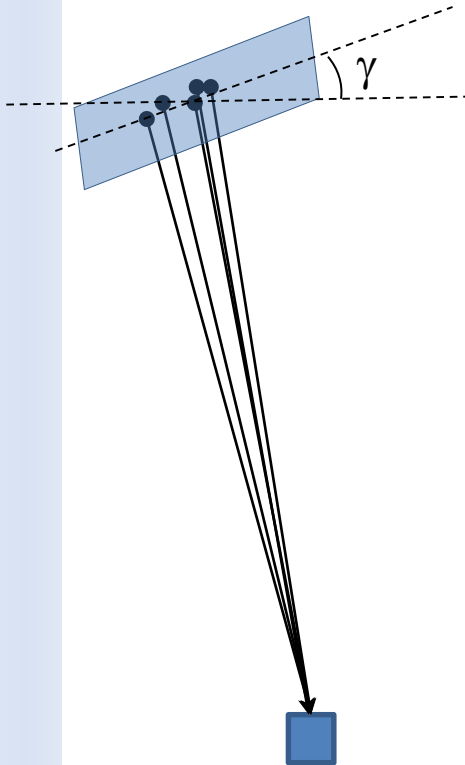


The transmitted signal illuminates a large area in the ionosphere, typically a few hundred kilometers in diameter (top). The transmitted radiowave reflects at every point in the ionosphere where the wave encounters the cut-off frequency (index of refraction is zero). If the normal to the surface of equal electron density points exactly towards the sounder, then the reflected signal can be detected by the system. Each such reflection point is considered as a “source” of a reflected signal. A map showing locations of all “sources” is called a “skymap” (right).



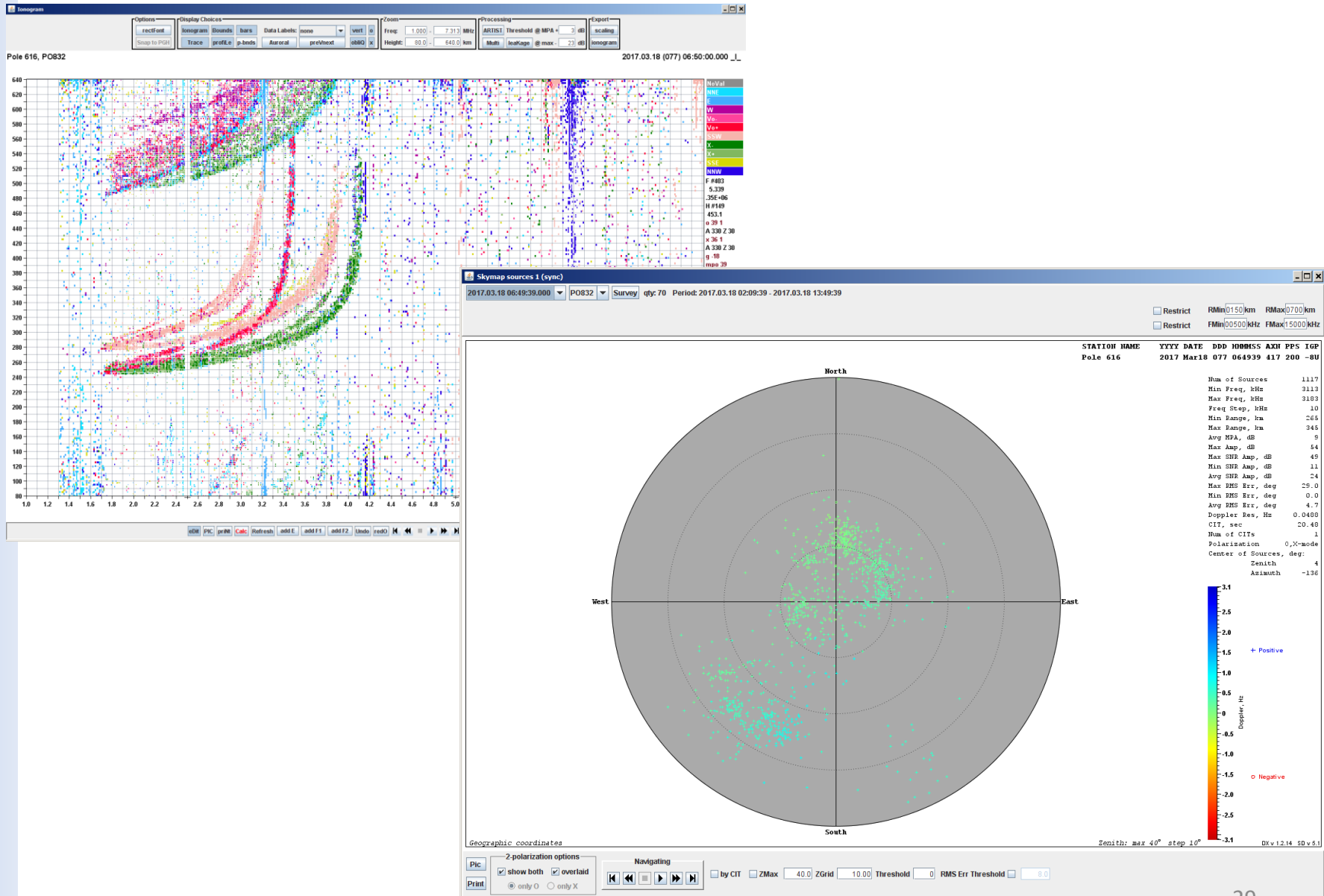


# Determining ionospheric tilt from skymap



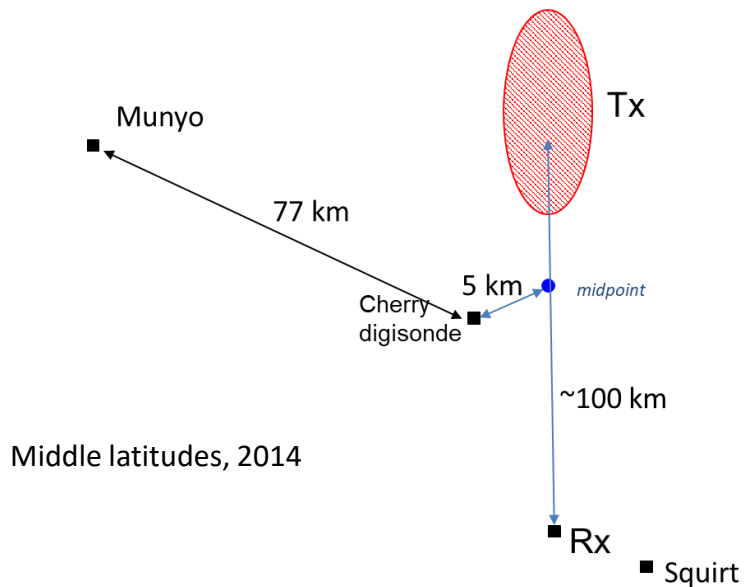
Ionospheric tilt angles specify the orientation of an imaginary surface (left) which reflects radiowaves to produce a specific skymap (right). Tilt angles are found as a “center-of-mass” of all the sources present in the skymap data.

# Example of strong persistent ionospheric tilt

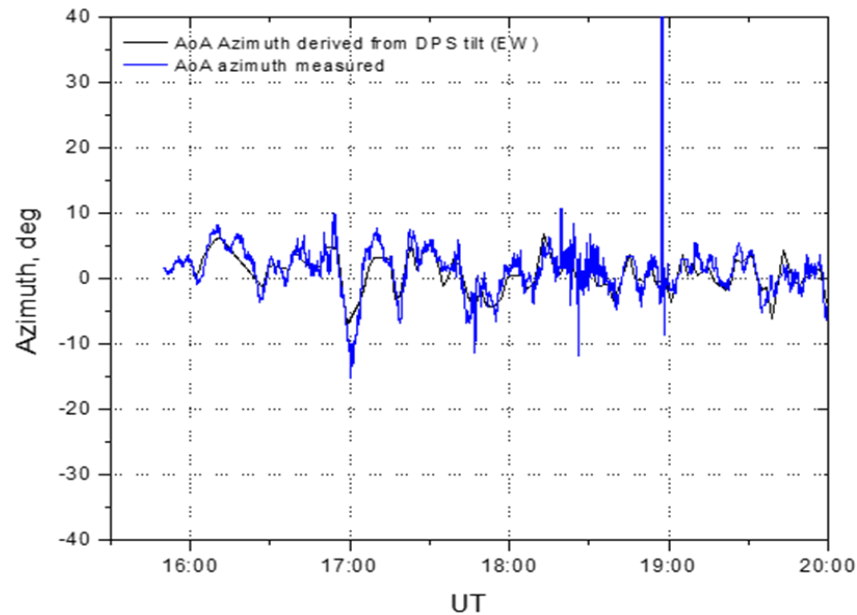
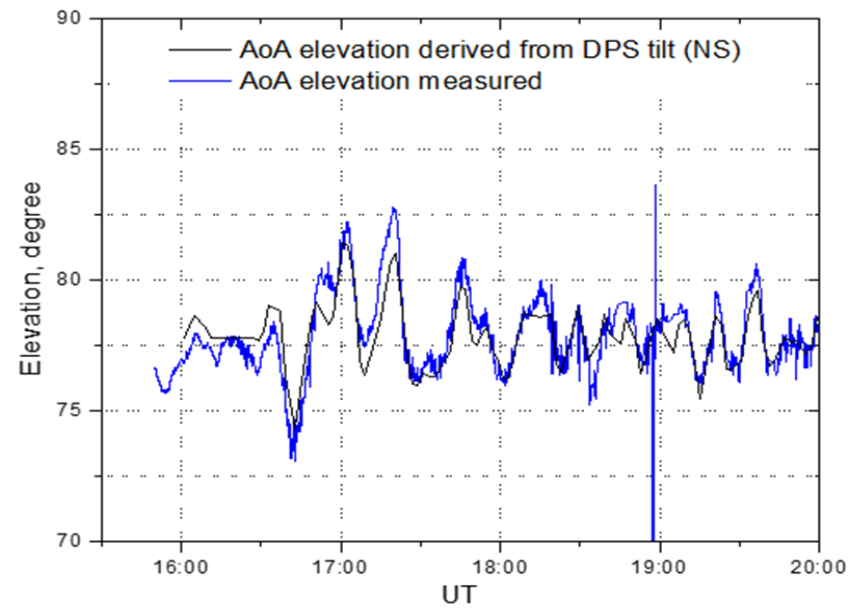




# Experimental proof of tilt concept

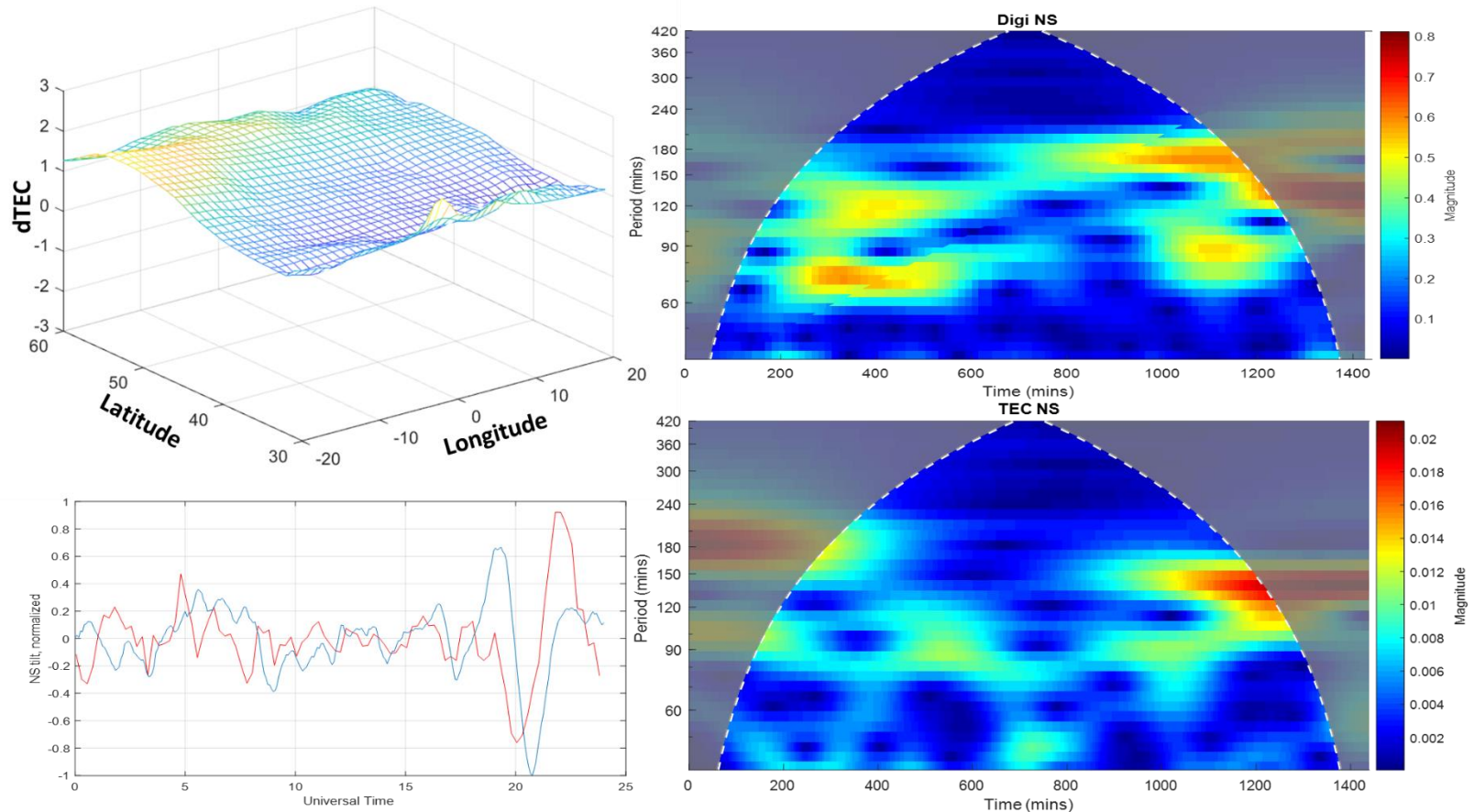


Using ionospheric tilt measurements near the midpoint of an HF link, it is possible to “reconstruct” AoA variations at the receive location. Top plot compares elevation angle measurements (blue) and reconstruction (black), and bottom one shows azimuthal angle comparison. This example shows AoA modelling with the use of the “mirror model” reflection and with the fixed reflection height, estimated from simultaneous ionogram measurements.





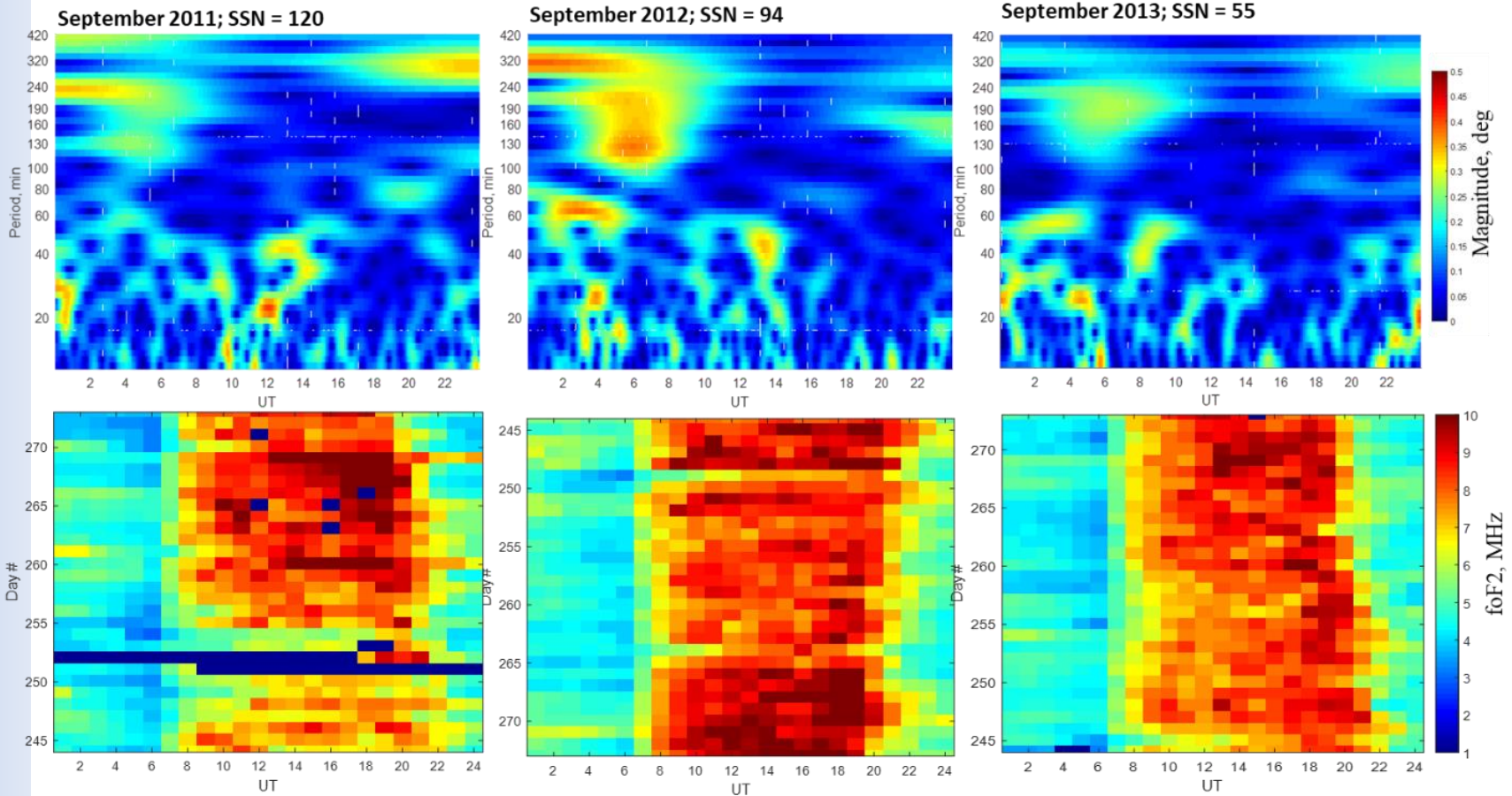
# Comparison to GNSS observations



Comparison of the tilts derived from digisonde and GNSS TEC measurements. Figure a) shows an example of the bottomside TEC map (effective surface) calculated using the network of the GNSS TEC receivers with the central point above Ebro Observatory. This snapshot is made for 21.9 UT on Apr 23, 2014. Figure b) shows a comparison of the North-South normalized tilt components calculated from the TEC map and measured with the Ebro digisonde. This correlation is also illustrated with the wavelet plots shown in part c).



# TIDs observations from tilt measurements

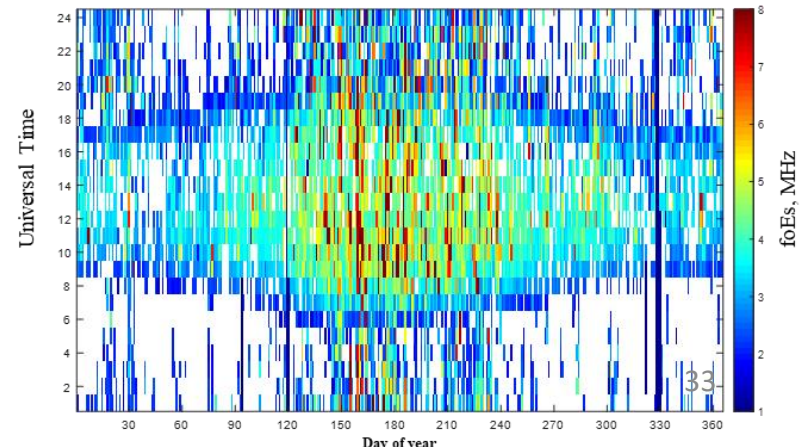
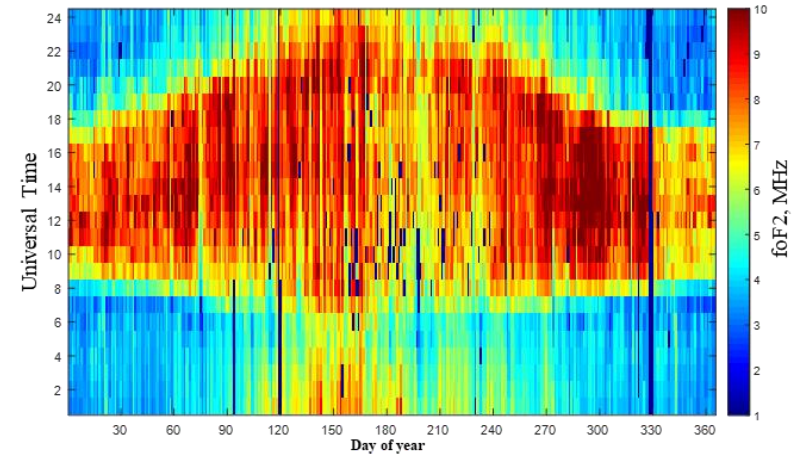
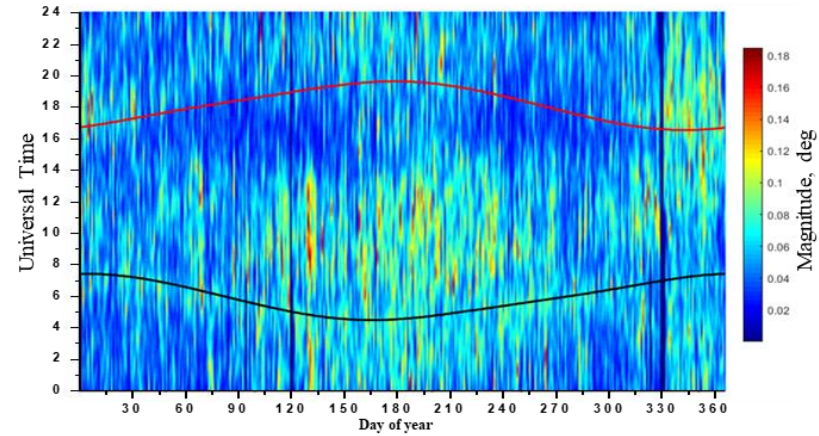


. Comparison of the tilt variations (NS-component) for different levels of solar activity during 2011-2013. Top row shows disturbance periods as a function of time a given month, bottom row shows corresponding background density distribution (in terms of foF2). There is no clear correlation between the intensity of the variations and the sun spot number (SSN), indicating that most of the variations are not of geomagnetic origin.





# TID climatology from tilt measurements

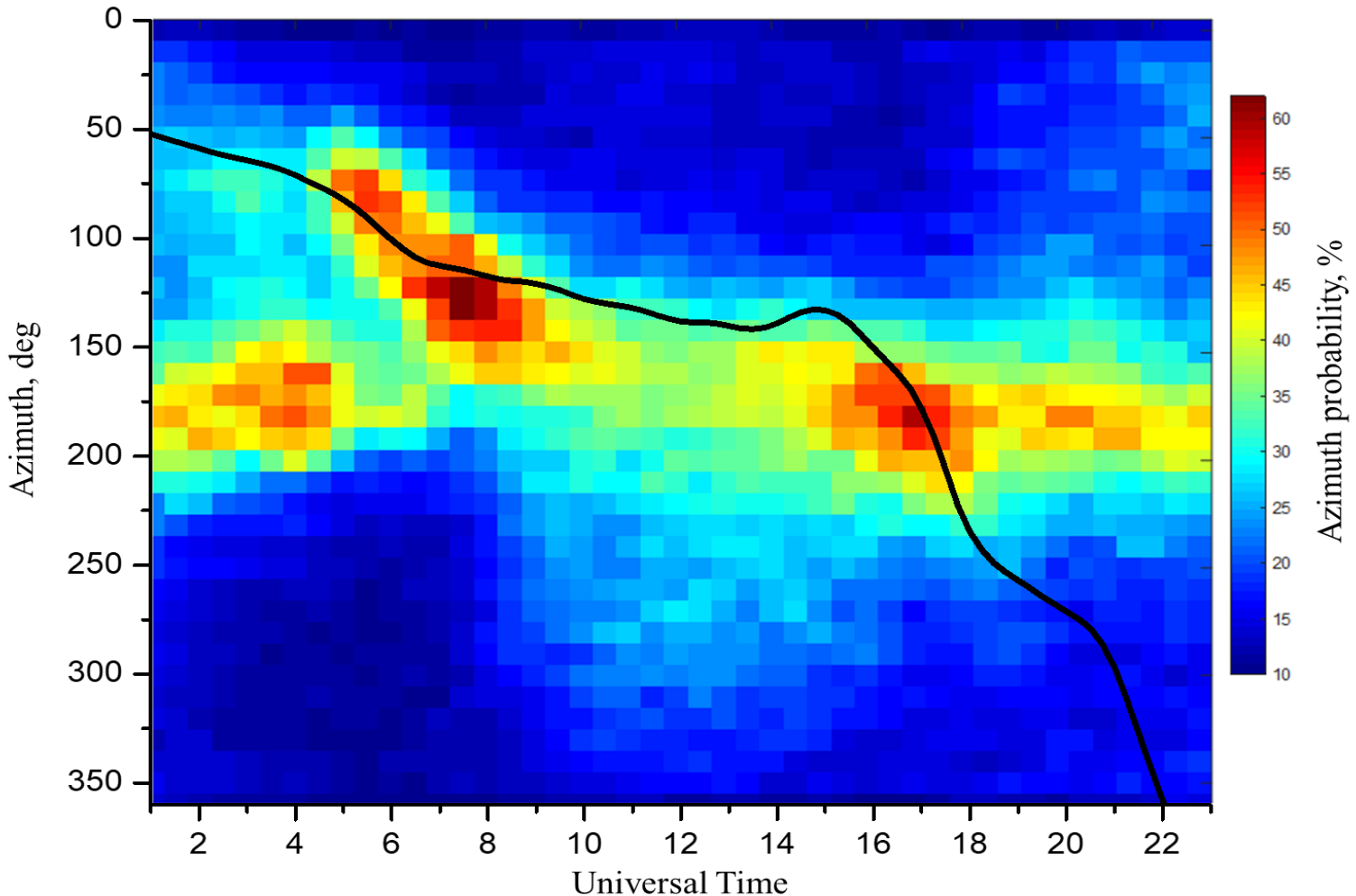


Top: Climatology of short period (20-80 min) variations for NS component calculated for 2012. The black and red line indicate the sunrise and sunset times (at ground level) correspondingly.

Middle: Plasma density distribution in terms of critical frequency, foF2. Bottom: Sporadic E layer occurrence at Ebro, showing the strongest sporadic layers present during the summertime period.



# TID propagation direction from tilt measurements



Distribution of the tilt azimuth (colormap) compared to the direction opposite to the neutral wind velocity (black line) for year 2012. Azimuthal direction of the tilt can be regarded as an indicator of the TID wave propagation direction (under the assumption of the plane wavefront).



# Conclusions from Ebro tilt observations

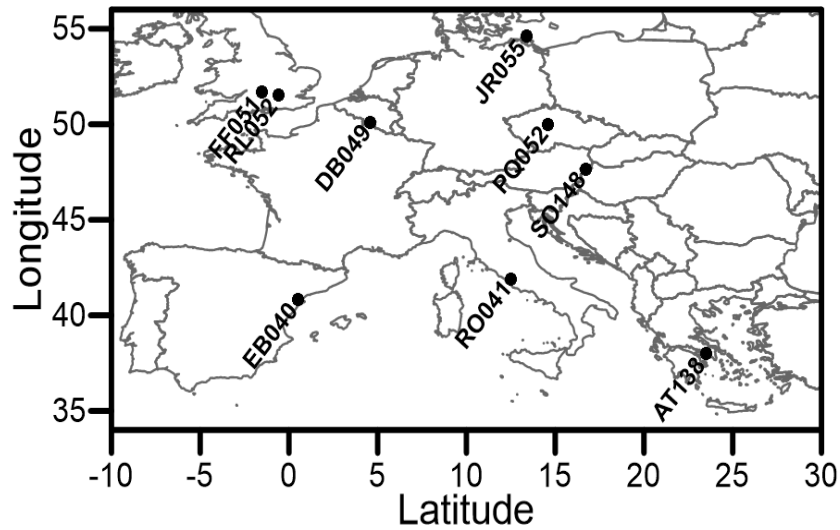
- **No visible effect of background plasma density on TID occurrence**
- **Possible link to sporadic Es presence**
- **Daytime TIDs propagate against background wind**
- **Nighttime TIDs predominantly propagate equatorward**
  
- **TID characteristics:**
  - Periods 20-80 min (more common for MSTIDs)**
- **More frequent during summertime**

[*Paznukhov et al.*, RS 2019, to be submitted]

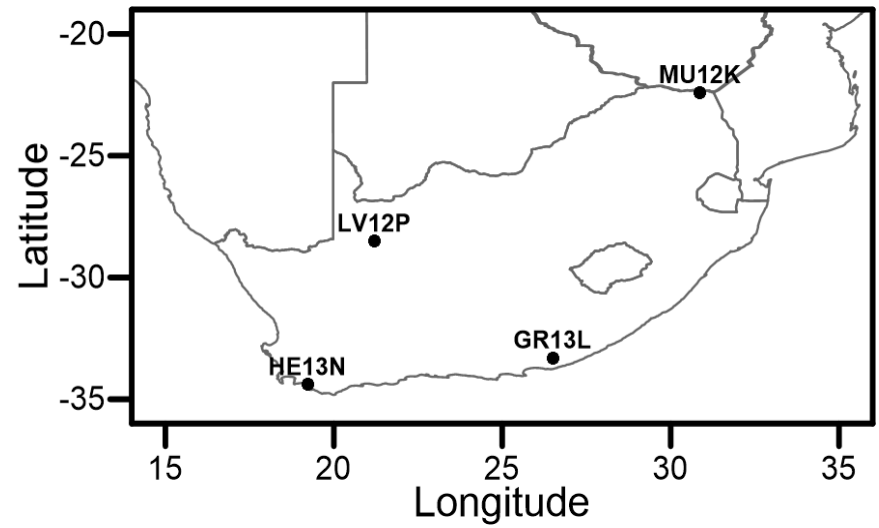


# HF interferometry

Europe (9 systems)

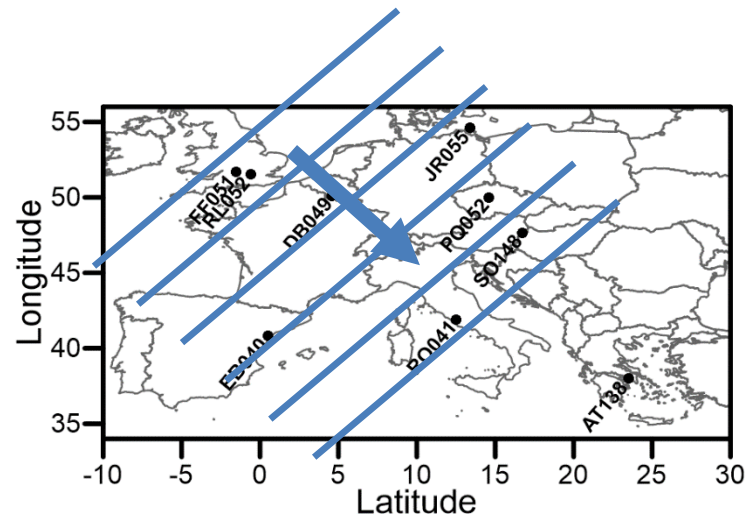


South Africa (4 systems)





# TID parameters calculations



For each  $i^{\text{th}}$  ionosonde station, the time delay  $\Delta t_i$  of the disturbance with respect to the reference station can be written as:

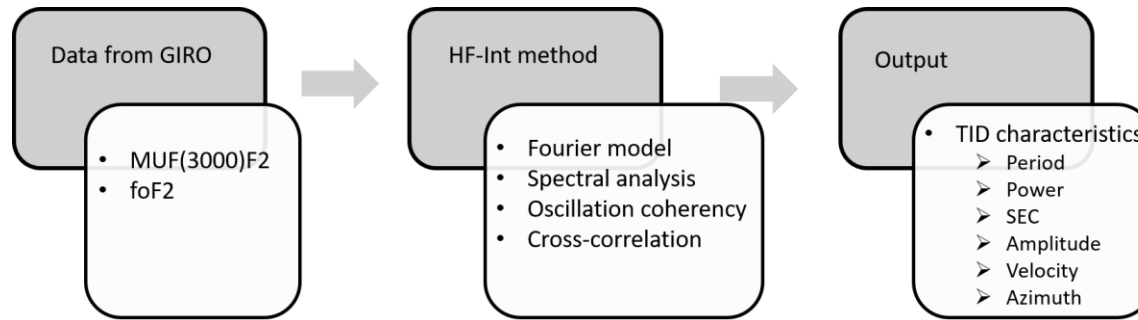
$$\Delta t_i = \vec{s} \cdot \Delta \vec{r}_i,$$

where  $\vec{s} = \vec{v}/v^2$  is the slowness vector of the disturbance propagating at velocity  $\vec{v}$ , which is an unknown variable;  $\Delta \vec{r}_i$  is the relative position vector of the  $i^{\text{th}}$  ionosonde with respect to the reference one.

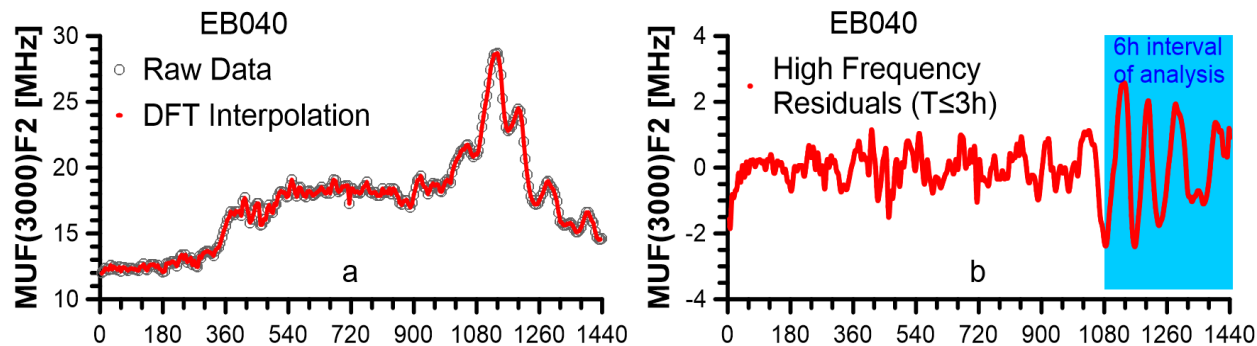
For a network of stations with  $i > 3$ , this system of equations is overdetermined and can be solved by a least squares fitting method.



# HF-Int processing chain



## Preprocessing



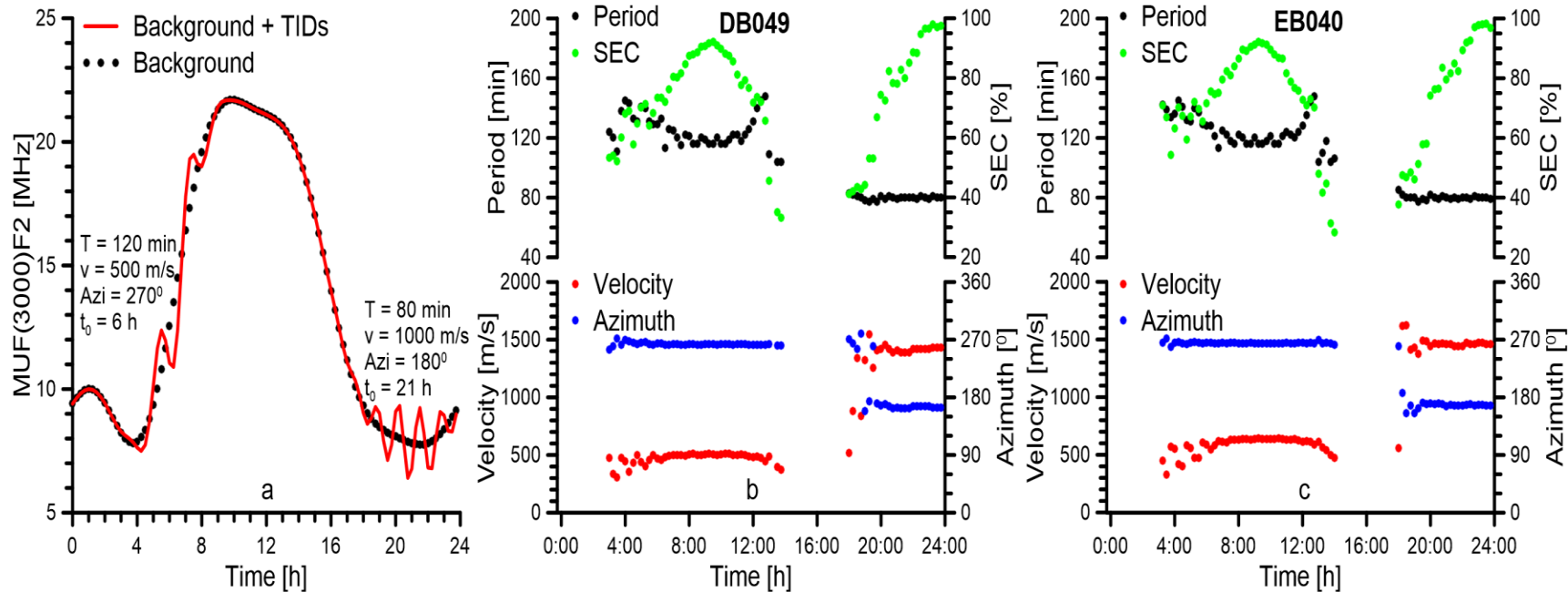
Calculation of the residuals for the detection of LSTID in the HF-Int method. Panel (a) compares the raw data with the DFT interpolated data and panel (b) depicts the residual values calculated by the contribution of the harmonics with  $T \leq 3h$

### Event selection criteria:

1. Confidence level above 0.975 at each site
2. Periods differ less than 30% at all sites
3. Consistent time delays and solution for all reference sites



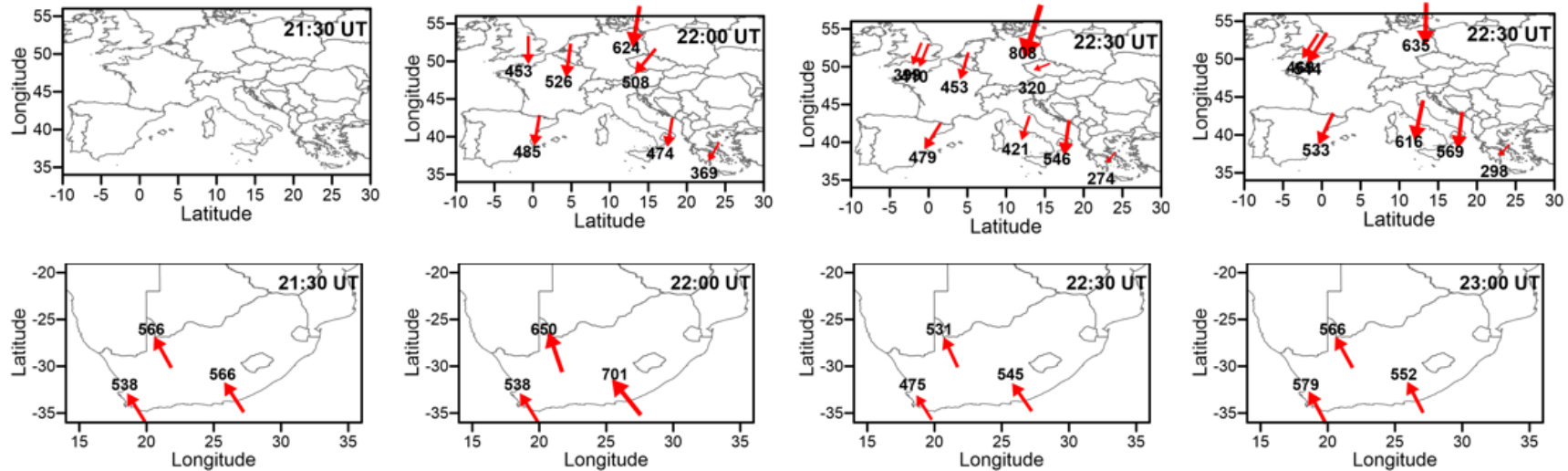
# HF-Int testing with simulated data



Verification of the HF-Int method with synthetic data. Panel a) shows simulated time variations of the MUF(3000)F2 for EB040 on 15 January 2017, with 2 TIDs events generated analytically (red line) with the indicated characteristics. Black dots correspond to the background calculated by IRI. Panels b) and c) show the results of the HF-Int method for DB049 and EB040 stations respectively.



# HF-Int validation results



Maps of the estimated velocity vectors of the LSTID event detected over Europe (top) and over South Africa (bottom) on 12 October 2015 for the indicated times.

Characteristics of the LSTID observed in Europe for the night of 12-13 October 2015 with independent methodologies and different data. Azimuth is counted clockwise from the true North .

Method	Period, T (min)	Velocity, V ( $\text{m}\cdot\text{s}^{-1}$ )	Azimuth ( $^{\circ}$ )	Wavelength, $\Lambda$ (km)
FAS	80	320	185	1536
GNSS	80	370	150	1776
HF-Int	80	400	205	1920

[Altadill et al., JSWSC, 2019 submitted]







# First HF-Int Observations Results

← → ↻ 🏠 Not secure | techtide.space.noa.gr/?page\_id=4467 🔍 ☆ D

📱 Apps 🌐 Agora Portal 📄 BC Application Serv... 📧 BC Email 📄 BC software 📄 BC Canvas 📄 Get Technology Help 🌐 Personal Web Server 📄 Safe Computing 📄 Real estate investin...



COMPET – Space Weather 2017  
Grant Agreement 776011

## TechTIDE Project

ber 2019, Prague, Czech Republic. [Click here!](#)

Home TID Activity Report Real-Time Conditions **Archive** Help

### Archive

**Warning:** The performance of the Archive page functionalities is currently verified with Chrome and Microsoft Edge browsers, while some incompatibilities are reported with Firefox!

Clear All Selections

See your selections here

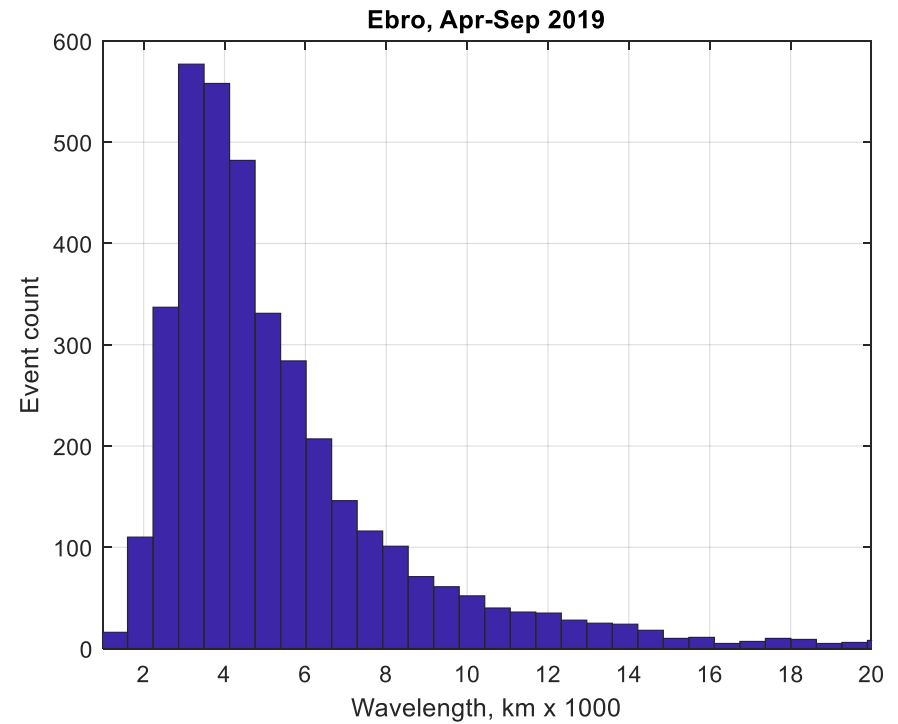
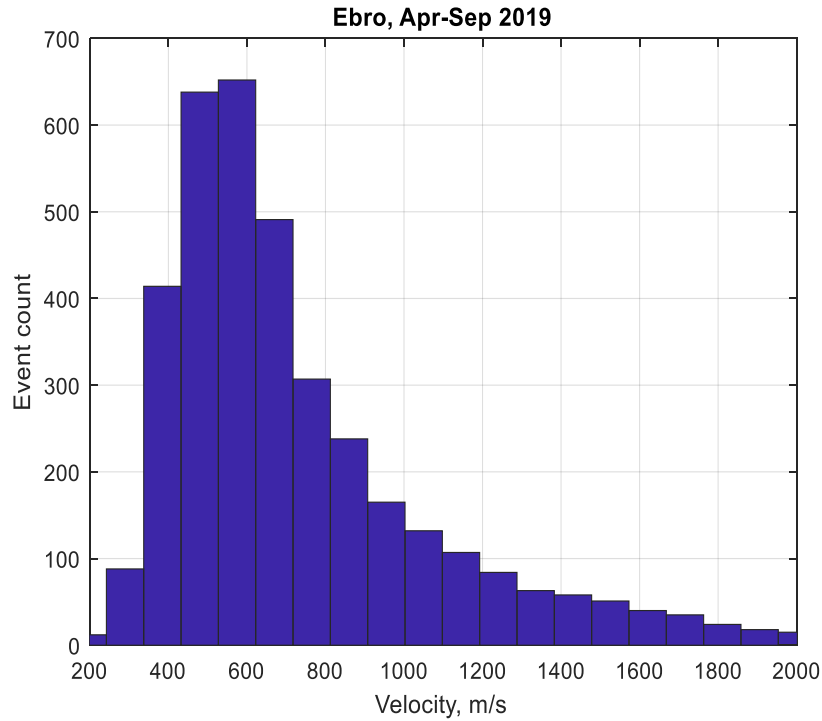
Selected start time: 2019-04-17 00:00 Selected end time: 2019-10-06 00:00 Selected product / supporting data set: Selected points of observation: Selected product results:

Make your selections here

Start Time Year: 2019 Month: 04 Day of the month: 17 Hour: 00 Minute: 00



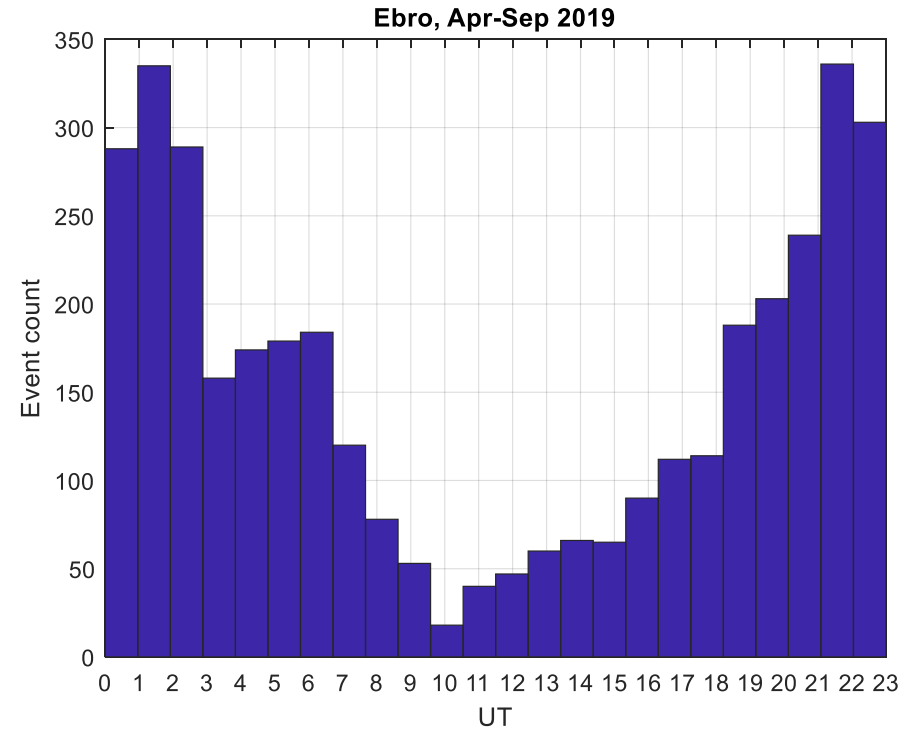
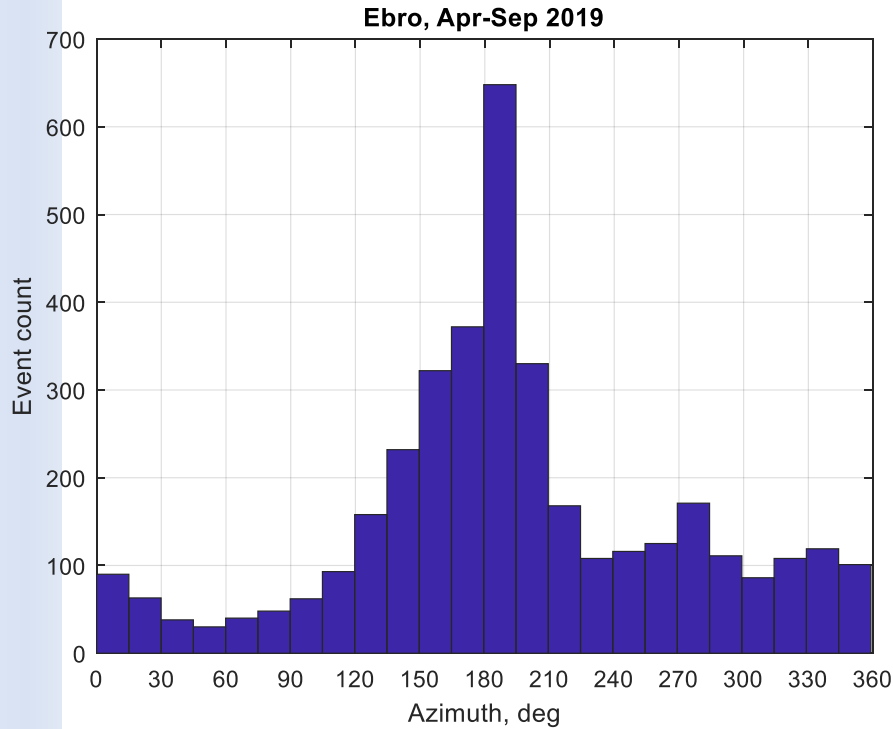
# TIDs parameters in Europe



LSTIDs are observed (determined by the method, i.e., very large spatial separation)



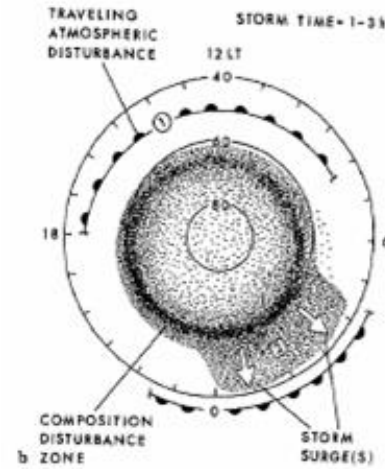
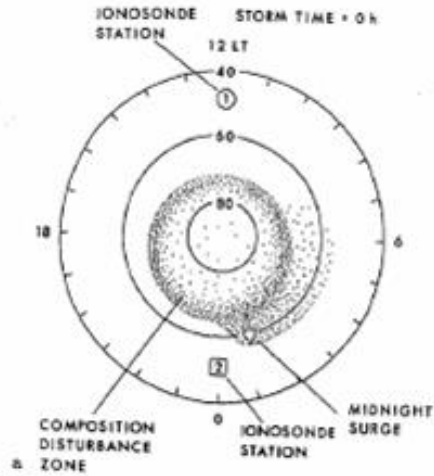
# TIDs parameters in Europe



Predominantly equatorward propagation of LSTIDs is observed with the clear maximum during the local midnight.  
Why so?

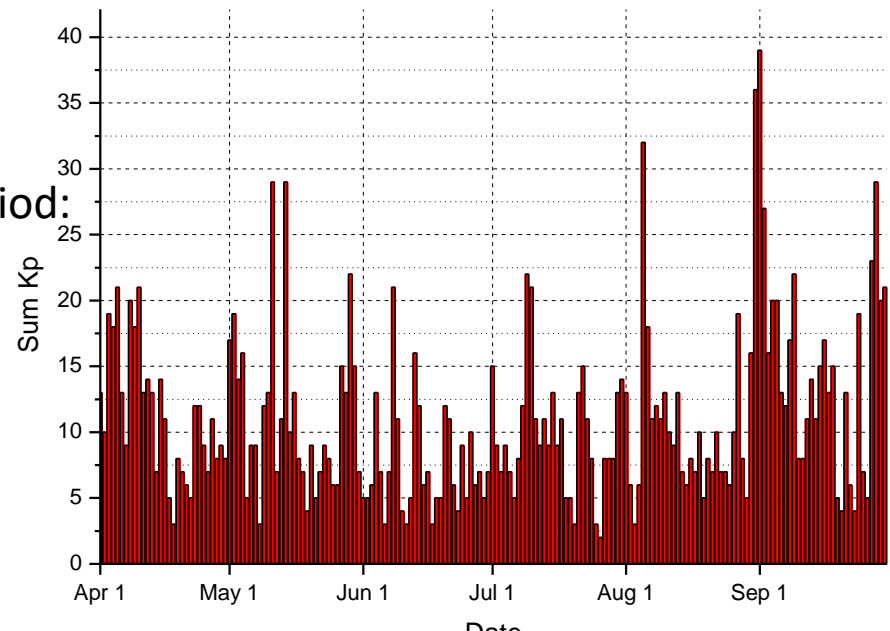


# Why midnight?



[Bates, 1977; Prolls, 1993]

But, April-September 2019 is a quiet period:





# First Results of TIDs observations with HF-Interferometry

- **Observations available for April-September 2019**
- **LSTIDs are observed about 15% of the time**
- **Very strong predominance of the equatorward propagation**
- **Well pronounced peak of the LSTIDs occurrence around local midnight.**
- **Are these LSTIDs originating in the auroral region?**



# Summary of TIDs observations in Antarctica and Europe

- **The most consistent is the fact of daytime TIDs propagation against background wind during the daytime. These are most likely MSTIDs produced “locally” in the troposphere below.**
- **Nighttime TIDs propagate equatorward. They are likely to be propagating from the auroral region, but there is no clear correlation with the geomagnetic activity.**
- **An alternative possibility for the nighttime TIDs are “electrified” TIDs.**
- **Events resulting from magnetosphere-ionosphere coupling are also observed.**